Heliyon 8 (2022) e09854

Contents lists available at ScienceDirect

Heliyon

journal homepage: www.cell.com/heliyon

Research article

Bioremoval of some heavy metals from aqueous solutions by two different indigenous fungi *Aspergillus* sp. AHM69 and *Penicillium* sp. AHM96 isolated from petroleum refining wastewater

Ahmed Mohamed Ahmed El-Bondkly [a,*], Mervat Morsy Abbas Ahmed El-Gendy [b]

[a] *Genetics and Cytology Department, National Research Centre, Dokki, Giza 12622, Egypt*
[b] *Chemistry of Natural and Microbial Products Department, National Research Centre, Dokki, Giza 12622, Egypt*

ARTICLE INFO

Keywords:
Fungal biosorbents
Heavy metals bioremoval
Oil refining industrial wastewater
Process optimization

ABSTRACT

Myco-remediation of heavy metals using indigenous fungi of different petroleum refining areas in Egypt was applied. Among the physicochemical parameters determined in these refineries effluents, the highest levels of heavy metals were recorded for the most toxic heavy metals Fe^{3+} and Co^{2+}. The fungal isolates under the isolation codes AHM69 and AHM96 isolated from the mycobiome of Mostorod and Tanta refineries, respectively showed the best bioremoval efficiency toward heavy metals from the real wastewater mixture and polycyclic aromatic hydrocarbons from aqueous solutions. Based on phenotypic and genotypic analysis they were identified as *Aspergillus* sp. AHM69 and *Penicillium* sp. AHM96. The optimum conditions for the best bioremoval of Fe^{3+} and Co^{2+} from aqueous solutions by *Aspergillus* sp. AHM69 were live biomass, temperature 45–55 °C, pH 4.5–5.0, contact time 180 min, metal concentration equal to 1000 and 400 mg/L of Fe^{3+} and Co^{2+} with live fungal biomass dose of 0.5% and 0.4% with Fe^{3+} and Co^{2+}, respectively. Concerning to the biomass of *Penicillium* sp. AHM96, the optimum operation conditions for the best removal of Fe^{3+} and Co^{2+} were 45 °C, pH 5.0 and 400 mg/L of Fe^{3+} with 1.0% biosorbent dosage or 1000 mg/L of Co^{2+} with 0.5% biosorbent dosage for 180 min as process time. Furthermore, FTIR analysis showed masking, shifting, creating and absenting of different functional groups in the fungal biomass surface of AHM96 and AHM69 strains in the presence of Fe^{3+} and Co^{2+} compared to unloaded biomasses. Microscopy with Energy Dispersive X-ray analysis (SEM-EDX) indicated that the removal of Fe^{3+} and Co^{2+} by fungi AHM69 and AHM96 was via biosorption and bioaccumulation on the biomass surface. Our results suggested that in the near future, fungal treatment is likely to outperform and replace other chemical and biological treatments in industrial wastewater treatment for oil refining.

1. Introduction

Water is the most critical natural resource for human survival. The world population is increasing day by day. Thus, to meet the increasing demand of the population, clean water is the main concern (Rekha and Lokeshappa, 2020). Under the prevailing conditions, wastewater reuse is an alternative to reduce misuse and encroachment on available natural water resources (El-Gendy and El-Bondkly, 2016). Wastewater from petroleum industries as oil production process, transportation, oil refinery, petrochemical products, storage and distribution consists of a variety of substances that are toxic to the environment and human health such as petroleum hydrocarbons, metals, phenol, mercaptans, oil and grease, sulfide and others (Raza et al., 2019). Heavy metals (HMs) as waste from different industries containing petroleum, leather, textile, pharmaceutical and others are the main pollutant existent in water are becoming one of the most serious environmental problems (Burakov et al., 2018; Kumar et al., 2019). They are classified as non-biodegradable pollutants and pose a particular threat to human health because of their potentially toxic or carcinogenic effects, and their resistant, persistent and accumulation nature in terrestrial and aquatic organisms (Pohl, 2020; Rekha and Lokeshappa, 2020). However, some of these heavy metals as iron and cobalt have functional roles that are necessary for different physiological and biochemical activities in the body, but in high doses they can be harmful to the body causing acute and chronic toxicity, neurotoxicity and generation of free radicals which stimulates oxidative stress that damage lipids, proteins and deoxyribonucleic acid (DNA) molecules (Engwa

* Corresponding author.
E-mail address: ahmed_bondkly@yahoo.com (A.M.A. El-Bondkly).

https://doi.org/10.1016/j.heliyon.2022.e09854
Received 11 December 2021; Received in revised form 19 February 2022; Accepted 28 June 2022

Table 1. Petroleum refining wastewater characteristics.

Parameter	Analysis in refining industrial wastewater (mg/L)			Water quality guidelines (allowable limit)					
	Mostorod (Cairo)	America (Alexandria)	Tanta (Delta)	Drinking water		groundwater		Irrigation[c]	Aquatic live[d]
				Egypt[a]	WHO[b]	Egypt[a]	WHO[b]		
Sodium (Na^+)	3214.21 ± 8.00	4160.73 ± 8.75	3000.39 ± 8.05	200	-	200	200	919	-
Potassium (K^+)	133.56 ± 3.12	140.18 ± 3.06	129.28 ± 3.40	2	-	10	10	-	-
Magnesium (Mg^{2+})	354.51 ± 1.39	320.15 ± 1.20	370.80 ± 1.50	150	-	150	150	60.0	-
Calcium (Ca^{2+})	554.20 ± 2.07	488.00 ± 1.90	480.13 ± 1.92	200	75	200	75	400	-
Aluminum (Al^{3+})	134.40 ± 1.26	173.90 ± 1.39	196.01 ± 1.17	0.2	0.2	-	-	5.0	0.1
Iron (Fe^{3+})	3250 ± 6.55	3085.45 ± 6.20	3452.41 ± 5.91	0.3	0.3	1.00	0.20	5.0	0.3
Manganese (Mn^{2+})	290.51 ± 0.91	281.40 ± 0.89	285.16 ± 0.80	0.1–0.5	0.4	0.1	0.5	0.2	0.050
Cupper (Cu^{2+})	16.89 ± 0.25	22.87 ± 0.21	20.34 ± 0.23	1.00	2	1.00	1.5	0.2	0.004
Zinc (Zn^{2+})	40.23 ± 0.29	32.59 ± 0.24	30.16 ± 0.26	5.0	0.5	3.00	5.00	2.0	0.050
Lead (Pb^{2+})	28.30 ± 0.31	26.17 ± 0.27	25.89 ± 0.36	0.050	0.010	0.05	0.01	5.0	0.007
Cobalt (Co^{2+})	291.61 ± 0.60	300.20 ± 0.75	289.74 ± 0.58	-	-	-	-	-	-
Nickel (Ni^{2+})	24.89 ± 0.24	22.90 ± 0.22	20.50 ± 0.21	0.020	0.070			0.2	0.025
Arsenic (As^{3+})	6.27 ± 0.11	6.20 ± 0.10	9.60 ± 0.15	0.05	0.01	-	-	-	-
Cadmium (Cd^{2+})	2.20 ± 0.05	3.73 ± 0.09	2.20 ± 0.07	0.005	0.003	0.005	0.003	0.010	0.010
Chromium (Cr^{6+})	9.18 ± 0.11	7.11 ± 0.14	5.83 ± 0.08	-	-	0.05	0.05	-	-
Boron (B^+)	68.42 ± 0.34	90.16 ± 0.45	71.16 ± 0.37	-	0.5	-	-	-	-
Barium (Ba^{2+})	180.32 ± 1.60	145.59 ± 1.53	195.80 ± 1.73	-	0.7	-	-	-	-
Silver (Ag^+)	2.19 ± 0.05	3.15 ± 0.12	2.50 ± 0.09	-	-	-	-	-	-
Mercury (Hg^{2+})	0.049 ± 0.003	0.057 ± 0.005	0.061 ± 0.005	0.001	0.001	-	-	-	-
Sulfate (SO_4^{2-})	70.13 ± 1.90	81.39 ± 1.04	92.61 ± 1.10	400	250	400	200	960	-
Chloride (Cl^-)	6310 ± 19.12	7500 ± 17.65	8227 ± 18.20	250	200	200	200	1063	120
NH_3–N	80.25 ± 2.70	71.00 ± 2.19	75.78 ± 2.83	<30	<30	<30	<30	<30	<30
NO_3–N	6.18 ± 0.74	5.83 ± 0.80	6.01 ± 0.85	-	-	-	-	-	-
Phosphorus (PO_4)	2.14 ± 0.90	3.26 ± 0.75	3.50 ± 0.88	<5	<5	<5	<5	<5	<5
Chemical oxygen demand (COD)	2520.34 ± 23.27	3150.00 ± 24.15	3000.71 ± 22.20	10.0	10.0	-	-	-	7.0
Biochemical oxygen demand (BOD5)	1081.12 ± 3.39	1382.58 ± 3.44	1279.60 ± 3.32	3.0	5	5	5	5	5
Total suspended solids (TSS)	750.62 ± 4.46	800.14 ± 5.12	780.06 ± 4.27	500	500	500	500	500	500
Total dissolved solids (TDS)	4095.39 ± 20.84	4240.61 ± 20.20	4183.52 ± 20.33	1000	500	1200	1000	2000	500
Benzene, toluene, xylene (BTX)	179.50 ± 1.95	162.21 ± 1.80	150.60 ± 2.13	-	-	-	-	-	-
Phenols	19.23 ± 2.21	20.40 ± 2.30	22.11 ± 2.54	-	-	-	-	-	-
Oil and grease	1682.95 ± 5.78	1643.00 ± 5.83	1690.87 ± 5.60	-	-	-	-	-	-
pH	2.50 ± 0.02	2.80 ± 0.02	2.70 ± 0.02	6.5–9.2	6.5–8.5	6.5–8.5	8.5	6.5–8.0	6.5–9.0
Electrical conductivity (EC μs/cm)	24,120 ± 30.69	19,237 ± 26.70	20,500 ± 28.16	2000	-	-	1500	3000	-
Turbidity (NTU)	400.0 ± 7.70	402 ± 7.80	419 ± 7.95	-	-	-	-	-	-
Color (Pt Co)	5526 ± 18.89	5409 ± 20.04	5655 ± 19.54	-	-	-	-	-	-

Not determined.

[a] Decree of Health Ministry (2007)

[b] WHO (2011)

[c] Ayers and Westcot (1994)

[d] Canadian Council of Ministers of the Environment 1999 (CCME 2007, 2011).

et al., 2019). Moreover, low-molecular-weight polycyclic aromatic hydrocarbons (PAHs) (comprising less than four benzene rings) are highly toxic and have effects on the reproduction and mortality rates for aquatic animals while high-molecular weight PAHs (comprising four or more benzene rings) are mutagenic, carcinogenic and bioaccumulate in food chains (Vahabisani and An, 2021).

Biosorption is defined as the removal of a substance from biological materials by live or dead biomass (Liu et al., 2018). Compared with other biosorption agents, fungi are a large and varied section of eukaryotic microorganisms. Their cell membrane consists of a thin, double-layered sheet of lipids, mainly with phospholipids and sterols (about 40% of membrane content) and protein molecules (about 60%), which reveals excellent heavy metals binding properties (Ayele et al., 2021). Filamentous fungi native to areas contaminated with heavy metals (HMs) have abundant bioremediation potential, yet they often remain untapped (El-Gendy et al., 2011, 2017; Sharma et al., 2022; Vacar et al., 2021). Many fungal-derived biomass of fungi as *Aspergillus niger*, *Penicillium brevicompactum*, *Termitomyces clypeatus*, *Penicillium simplicissimum*, *Aspergillus fumigatus*, *Saccharomyces cerevisiae* are widely applied as sorbents for heavy metals and other pollutants from wastewater because of their high adsorption capability and affinity, low cost, selectivity, their availability in large quantities and their eco-friendly nature however the another techniques have inherent restrictions such as large amount of sludge generation, sensitive operating conditions, low efficiency and costly disposal (Rastegari et al., 2019). Fourier-transform infrared spectroscopy (FTIR), scanning electron microscopy (SEM) and energy-dispersive X-ray spectroscopy (EDX) are good tools for analyzing the functional groups, specified chemical element or providing partial multi-element analysis to conclude elemental composition profiles and toxic heavy metals in fungal biomass on the basis of fungal uptake (Scimeca et al., 2018). Current research was designated to, (1) analyses of the physical and chemical characteristics of the petroleum refining industrial wastewater obtained from different drainage areas in Egypt, (2) evaluation of the bioremediation capacity of different indigenous fungi

Table 2. Bioremoval efficiency (%) of different pollutants by the live biomass of mycobiome derived from the oily effluents.

Pollutants*	Removal efficiencies of fungal isolates (%)																			
	AHM50	AHM55	AHM60	AHM65	AHM69	AHM70	AHM75	AHM80	AHM85	AHM90	AHM96	AHM100	AHM105	AHM110	AHM115	AHM120	AHM125	AHM130	AHM135	AHM140
Na^{+}	70.11 ± 0.70	83.19 ± 0.26	48.20 ± 0.52	64.15 ± 0.43	90.85 ± 0.85	71.0 ± 0.63	80.35 ± 0.74	50.08 ± 0.60	60.59 ± 1.03	51.21 ± 0.94	84.32 ± 1.10	67.15 ± 1.00	80.28 ± 1.16	52.60 ± 0.89	47.20 ± 0.61	78.28 ± 1.06	71.90 ± 1.03	49.00 ± 0.70	63.51 ± 0.92	82.37 ± 1.22
K^{+}	51.26 ± 0.66	80.45 ± 0.55	60.18 ± 0.66	73.13 ± 0.72	69.18 ± 0.74	70.62 ± 0.86	60.74 ± 0.52	58.24 ± 0.64	33.90 ± 0.50	50.30 ± 0.70	78.90 ± 0.81	50.63 ± 0.65	32.70 ± 0.48	50.19 ± 0.38	40.15 ± 0.31	43.71 ± 0.31	60.18 ± 0.52	28.73 ± 0.24	51.20 ± 0.42	37.40 ± 0.30
Mg^{2+}	67.10 ± 0.37	50.59 ± 0.42	44.29 ± 0.47	50.28 ± 0.40	58.06 ± 0.24	42.90 ± 0.47	48.56 ± 0.50	58.90 ± 0.47	50.63 ± 0.40	42.23 ± 0.35	69.54 ± 0.50	18.42 ± 0.20	40.31 ± 0.39	54.60 ± 0.39	39.60 ± 0.34	62.17 ± 0.51	70.31 ± 0.52	51.49 ± 0.40	37.64 ± 0.29	45.60 ± 0.36
Ca^{2+}	84.15 ± 0.40	64.35 ± 0.39	89.15 ± 0.50	68.30 ± 0.51	90.66 ± 0.50	71.54 ± 0.39	50.80 ± 0.30	60.25 ± 0.35	56.80 ± 0.31	60.30 ± 0.29	84.30 ± 0.32	66.09 ± 0.22	78.32 ± 0.34	80.00 ± 0.39	36.40 ± 0.18	70.31 ± 0.33	61.15 ± 0.26	44.00 ± 0.23	82.05 ± 0.40	39.02 ± 0.19
Al^{3+}	90.17 ± 0.60	51.83 ± 0.49	22.60 ± 0.30	61.14 ± 0.42	100.0 ± 0.50	70.80 ± 0.54	63.42 ± 0.40	76.00 ± 0.48	50.41 ± 0.48	39.64 ± 0.34	94.22 ± 0.61	55.82 ± 0.61	40.38 ± 0.56	83.10 ± 0.59	42.11 ± 0.38	90.02 ± 0.66	64.26 ± 0.50	29.80 ± 0.22	50.17 ± 0.42	69.28 ± 0.58
Fe^{3+}	20.41 ± 0.60	8.90 ± 0.37	43.05 ± 0.50	30.16 ± 0.50	100.0 ± 0.60	33.60 ± 0.40	30.50 ± 0.45	36.21 ± 0.50	20.28 ± 0.44	31.36 ± 0.29	51.77 ± 0.40	11.45 ± 0.19	24.00 ± 0.20	33.05 ± 0.27	16.50 ± 0.10	35.23 ± 0.26	40.15 ± 0.31	10.58 ± 0.13	24.17 ± 0.24	40.19 ± 0.36
Mn^{2+}	93.63 ± 0.50	70.13 ± 0.30	42.65 ± 0.32	100.0 ± 0.50	100.0 ± 0.80	80.70 ± 0.80	61.30 ± 0.70	79.03 ± 0.40	75.00 ± 0.48	70.52 ± 0.40	90.00 ± 0.29	72.13 ± 0.16	60.18 ± 0.40	50.31 ± 0.36	48.16 ± 0.49	75.90 ± 0.58	66.53 ± 0.50	84.82 ± 0.60	90.41 ± 0.58	48.00 ± 0.42
Cu^{2+}	100.0 ± 0.60	60.50 ± 0.61	56.99 ± 0.70	55.26 ± 0.72	97.10 ± 0.66	74.12 ± 0.87	88.89 ± 0.87	80.92 ± 0.63	43.49 ± 0.50	35.34 ± 0.57	89.81 ± 0.70	90.11 ± 0.71	62.00 ± 0.50	55.11 ± 0.61	70.32 ± 0.60	90.22 ± 0.85	80.30 ± 0.66	61.14 ± 0.50	59.00 ± 0.48	100.0 ± 0.00
Zn^{2+}	79.04 ± 0.30	80.30 ± 0.29	60.22 ± 0.34	100.0 ± 0.00	100.0 ± 0.24	90.00 ± 0.19	64.57 ± 0.18	100.0 ± 0.14	84.00 ± 0.16	70.29 ± 0.13	100.0 ± 0.09	88.10 ± 0.19	100.0 ± 0.00	79.02 ± 0.08	98.00 ± 0.20	69.40 ± 0.19	57.31 ± 0.11	75.60 ± 0.23	100.0 ± 0.00	100.0 ± 0.00
Pb^{2+}	58.71 ± 0.14	63.64 ± 0.27	71.00 ± 0.38	60.42 ± 0.23	100.0 ± 0.84	90.44 ± 0.47	100.0 ± 0.09	60.00 ± 0.17	52.00 ± 0.15	86.47 ± 0.15	100.0 ± 0.06	53.52 ± 0.05	59.50 ± 0.03	66.24 ± 0.08	91.68 ± 0.01	62.94 ± 0.0	84.29 ± 0.37	73.05 ± 0.29	64.28 ± 0.05	93.85 ± 0.32
Co^{2+}	11.40 ± 0.16	18.71 ± 0.13	23.14 ± 0.18	20.10 ± 0.16	50.22 ± 0.25	15.30 ± 0.13	23.00 ± 0.19	10.46 ± 0.05	3.27 ± 0.00	4.00 ± 0.00	100.0 ± 0.29	6.52 ± 0.00	19.00 ± 0.17	42.17 ± 0.28	21.40 ± 0.22	35.27 ± 0.06	40.11 ± 0.23	16.69 ± 0.18	29.08 ± 0.19	43.20 ± 0.27
Ni^{2+}	91.56 ± 0.88	79.21 ± 0.80	100.0 ± 0.76	80.33 ± 0.87	100.0 ± 0.84	90.52 ± 0.94	68.34 ± 0.70	80.50 ± 0.84	70.56 ± 0.83	100.0 ± 0.16	82.59 ± 0.90	100.0 ± 0.58	60.10 ± 0.70	72.80 ± 0.83	100.0 ± 0.63	51.40 ± 0.49	.100.0 ± 0.59	58.10 ± 0.42	55.20 ± 0.54	100.0 ± 0.61
As^{3+}	19.72 ± 0.59	25.62 ± 0.28	70.04 ± 0.41	30.18 ± 0.36	100.0 ± 0.64	27.61 ± 0.30	83.00 ± 0.48	50.13 ± 0.42	62.82 ± 0.31	65.81 ± 0.20	90.00 ± 0.26	100.0 ± 0.60	22.19 ± 0.11	71.30 ± 0.26	84.24 ± 0.33	29.47 ± 0.16	50.14 ± 0.29	64.00 ± 0.23	93.17 ± 0.40	100.0.±0.60
Cd^{2+}	90.02 ± 0.70	90.40 ± 0.81	30.83 ± 0.59	70.23 ± 0.80	75.83 ± 0.90	61.40 ± 0.87	58.75 ± 0.69	80.10 ± 0.81	81.40 ± 0.87	78.13 ± 0.80	100.0 ± 0.75	35.91 ± 0.18	100.0 ± 0.66	75.90 ± 0.71	90.16 ± 0.76	100.0 ± 0.59	60.18 ± 0.47	54.33 ± 0.23	40.65 ± 0.38	100.0 ± 0.60
Cr^{6+}	50.17 ± 0.70	48.00 ± 0.54	90.32 ± 0.80	70.02 ± 0.60	84.54 ± 0.60	80.00 ± 0.64	58.30 ± 0.70	100.0 ± 1.00	56.26 ± 0.71	90.9 ± 1.02	100.0 ± 0.84	80.45 ± 0.95	48.38 ± 0.61	100.0 ± 0.89	63.75 ± 0.78	86.20 ± 0.91	100.0 ± 0.79	73.00 ± 0.69	100.0 ± 0.80	44.15 ± 0.40
SO_4^{2-}	68.48 ± 0.90	51.60 ± 0.58	50.40 ± 0.55	60.31 ± 0.59	71.2 ± 0.92	60.24 ± 0.60	63.27 ± 0.54	70.23 ± 0.65	61.59 ± 0.96	50.46 ± 0.77	68.93 ± 1.02	38.82 ± 0.48	50.17 ± 0.52	79.00 ± 0.69	60.29 ± 0.71	40.21 ± 0.50	71.05 ± 1.00	68.14 ± 0.88	40.10 ± 0.37	66.50 ± 0.80
Cl^{-}	69.40 ± 0.55	80.65 ± 0.70	53.44 ± 0.62	70.02 ± 0.76	91.2 ± 0.86	76.21 ± 0.70	90.00 ± 0.83	59.66 ± 0.67	68.73 ± 0.63	60.13 ± 0.58	90.57 ± 0.91	74.00 ± 0.69	85.41 ± 0.73	60.78 ± 0.56	51.18 ± 0.44	84.00 ± 0.78	76.11 ± 0.73	55.00 ± 0.60	70.51 ± 0.62	90.00 ± 1.03
TPHs	78.29 ± 0.82	78.18 ± 0.66	85.00 ± 0.69	80.40 ± 0.80	98.15 ± 1.22	86.50 ± 0.87	70.82 ± 0.63	84.12 ± 0.76	53.80 ± 0.60	80.00 ± 0.82	99.20 ± 0.91	56.03 ± 0.52	87.53 ± 0.70	94.15 ± 0.86	75.11 ± 0.58	82.96 ± 0.88	75.13 ± 0.65	98.00 ± 0.90	50.73 ± 0.64	82.46 ± 0.85
PAHs	81.56 ± 0.92	80.25 ± 0.60	81.42 ± 0.73	90.13 ± 0.80	99.91 ± 1.16	83.31 ± 0.90	68.00 ± 0.59	90.00 ± 0.83	60.25 ± 0.75	77.25 ± 0.70	98.26 ± 0.86	64.20 ± 0.63	80.93 ± 0.69	88.60 ± 0.71	81.60 ± 0.71	94.00 ± 0.80	69.06 ± 0.60	90.25 ± 0.65	57.90 ± 0.48	100.0 ± 0.54
BOD	75.33 ± 0.84	70.04 ± 0.72	84.31 ± 0.76	76.68 ± 0.66	98.00 ± 0.55	79.42 ± 0.62	65.12 ± 0.47	83.20 ± 0.63	50.88 ± 0.40	73.00 ± 0.49	94.91 ± 0.50	70.16 ± 0.50	88.90 ± 0.60	77.58 ± 0.48	79.05 ± 0.54	90.17 ± 0.62	95.82 ± 0.68	94.49 ± 0.61	80.00 ± 0.57	90.30 ± 0.41
TOC	70.18 ± 0.56	68.71 ± 0.44	80.84 ± 0.65	70.93 ± 0.70	90.80 ± 1.14	68.24 ± 0.40	58.10 ± 0.54	71.56 ± 0.61	43.00 ± 0.37	81.28 ± 0.50	85.06 ± 0.39	60.52 ± 0.40	83.13 ± 0.40	76.90 ± 0.34	72.90 ± 0.29	88.22 ± 0.47	80.25 ± 0.37	87.12 ± 0.32	70.94 ± 0.20	81.17 ± 0.53
COD	63.73 ± 0.69	59.40 ± 0.29	68.88 ± 0.59	65.26 ± 0.60	97.25 ± 0.80	76.51 ± 0.67	61.13 ± 0.37	69.92 ± 0.37	55.93 ± 0.21	86.13 ± 0.50	95.80 ± 0.35	67.21 ± 0.32	80.01 ± 0.30	84.00 ± 0.32	70.04 ± 0.21	70.32 ± 0.26	97.91 ± 0.40	93.4 ± 0.46	64.76 ± 0.30	82.30 ± 0.47
BTX	71.80 ± 0.59	80.11 ± 0.38	66.00 ± 0.39	74.25 ± 0.30	90.31 ± 0.42	68.08 ± 0.50	54.18 ± 0.40	60.04 ± 0.29	50.00 ± 0.20	76.19 ± 0.35	85.76 ± 0.31	52.99 ± 0.16	73.52 ± 0.30	67.50 ± 0.21	60.41 ± 0.30	70.58 ± 0.40	64.04 ± 0.29	82.73 ± 0.35	42.86 ± 0.13	83.16 ± 0.45
TSS	84.14 ± 0.28	80.00 ± 0.33	84.90 ± 0.29	80.32 ± 0.40	99.20 ± 0.53	82.50 ± 0.24	62.17 ± 0.27	68.47 ± 0.19	58.27 ± 0.24	82.70 ± 0.30	98.00 ± 0.22	84.95 ± 0.28	97.65 ± 0.31	83.4 ± 0.29	70.55 ± 0.36	80.00 ± 0.32	76.69 ± 0.31	90.06 ± 0.41	63.06 ± 0.25	78.06 ± 0.41
TDS	86.10 ± 0.57	88.10 ± 0.62	79.70 ± 0.51	86.41 ± 0.58	95.12 ± 0.60	80.85 ± 0.57	71.12 ± 0.60	75.18 ± 0.49	63.90 ± 0.54	80.20 ± 0.63	96.40 ± 0.72	78.19 ± 0.56	89.10 ± 0.70	80.64 ± 0.50	81.14 ± 0.54	88.19 ± 0.60	83.90 ± 0.49	79.99 ± 0.65	59.80 ± 0.41	80.30 ± 0.50
Phenols	80.90 ± 0.78	73.54 ± 0.90	68.27 ± 0.80	90.0 ± 0.74	97.00 ± 0.90	90.20 ± 1.00	58.90 ± 0.92	68.24 ± 0.84	60.51 ± 0.63	70.51 ± 1.05	90.11 ± 1.02	50.27 ± 0.69	39.80 ± 0.59	79.34 ± 0.89	90.31 ± 0.95	70.65 ± 0.83	69.22 ± 0.70	58.36 ± 0.64	54.62 ± 0.67	82.60 ± 0.90
Turbidity	66.20 ± 0.49	68.77 ± 0.54	70.21 ± 0.80	65.00 ± 0.60	87.31 ± 0.60	69.00 ± 0.54	46.20 ± 0.49	60.15 ± 0.62	64.90 ± 0.58	70.13 ± 0.71	89.0 ± 0.69	68.35 ± 0.51	80.15 ± 0.70	70.18 ± 0.75	78.00 ± 0.89	80.05 ± 0.81	69.95 ± 0.66	84.01 ± 0.63	68.19 ± 0.45	600.35 ± 0.46
Oil and grease	87.00 ± 1.01	82.15 ± 0.81	90.15 ± 0.92	90.62 ± 0.89	98.15 ± 1.12	80.62 ± 0.87	70.15 ± 0.90	84.20 ± 0.88	73.92 ± 0.93	88.30 ± 0.89	99.10 ± 0.96	90.14 ± 1.00	81.60 ± 1.05	75.41 ± 0.82	69.48 ± 0.70	88.60 ± 1.12	72.00 ± 0.81	68.96 ± 0.90	93.16 ± 1.22	59.02 ± 0.65
Total nitrogen	80.16 ± 0.73	80.20 ± 0.75	76.52 ± 0.61	82.43 ± 0.77	92.50 ± 0.46	68.08 ± 0.32	89.37 ± 0.87	60.80 ± 0.63	90.80 ± 0.17	69.16 ± 0.34	94.4 ± 0.59	90.22 ± 0.65	55.16 ± 0.23	60.53 ± 0.28	74.61 ± 0.33	80.15 ± 0.34	87.39 ± 0.40	83.35 ± 0.32	72.35 ± 0.42	60.20 ± 0.48
Total phosphorus	72.40 ± 0.51	66.19 ± 0.40	81.00 ± 0.50	70.11 ± 0.46	90.20 ± 0.70	86.16 ± 0.61	78.24 ± 0.55	56.60 ± 0.35	74.00 ± 0.41	75.32 ± 0.44	88.21 ± 0.51	70.00 ± 0.51	75.46 ± 0.32	83.08 ± 0.45	60.29 ± 0.44	90.00 ± 0.71	65.83 ± 0.50	47.01 ± 0.30	68.70 ± 0.33	52.14 ± 0.21
Color (Pt Co)	68.13 ± 0.37	50.44 ± 0.21	76.20 ± 0.41	66.92 ± 0.31	89.84 ± 0.45	71.14 ± 0.30	80.00 ± 0.45	68.12 ± 0.28	50.43 ± 0.21	60.19 ± 0.31	93.10 ± 0.52	80.00 ± 0.81	77.63 ± 0.91	64.50 ± 0.52	90.02 ± 1.04	57.10 ± 0.49	88.32 ± 1.06	66.15 ± 0.80	40.25 ± 0.61	53.18 ± 0.51

* TPHs = total petroleum hydrocarbons, PAHs = polycyclic aromatic hydrocarbons, BOD = biochemical oxygen demand, TOC = total organic carbon, COD = chemical oxygen demand, BTX= (benzene; toluene; xylene), TSS = total suspended solids, TDS = total dissolved solids.

Table 3. Bioadsorption efficiency (%) of PAHs from the aqueous solution by the live biomass of mycobiome derived from the oily effluents.

Strain	PAHs								
	Acenaphthylene	Acenaphthene	Phenanthrene	Anthracene	Fluoranthene	Pyrene	Benz[a] anthracene	Chrysene	Benzo[a] pyrene
	Adsorption efficiency (%)								
AHM50	20.38 ± 0.44	18.40 ± 0.28	26.19 ± 0.13	75.38 ± 1.28	72.28 ± 0.62	60.32 ± 1.52	58.00 ± 0.94	70.18 ± 1.20	25.10 ± 0.81
AHM55	45.10 ± 0.70	23.51 ± 0.34	38.20 ± 0.25	66.14 ± 1.16	75.18 ± 0.66	72.00 ± 1.59	63.37 ± 1.15	50.69 ± 0.80	56.22 ± 1.59
AHM60	28.19 ± 0.49	40.16 ± 0.57	65.11 ± 0.45	50.16 ± 0.86	81.40 ± 0.71	59.50 ± 1.46	44.18 ± 0.80	72.44 ± 1.14	73.15 ± 1.90
AHM65	61.22 ± 0.88	35.28 ± 0.51	60.71 ± 0.49	41.72 ± 0.75	66.85 ± 0.50	64.30 ± 1.55	60.10 ± 0.99	46.00 ± 0.73	18.68 ± 0.60
AHM69	83.55 ± 1.24	80.90 ± 0.95	84.31 ± 0.69	90.25 ± 1.34	80.60 ± 0.80	72.14 ± 1.74	69.20 ± 1.06	79.99 ± 1.40	63.71 ± 1.89
AHM70	40.17 ± 0.63	60.21 ± 0.62	30.90 ± 0.19	71.14 ± 1.22	90.50 ± 0.80	70.19 ± 1.67	51.11 ± 0.90	70.48 ± 1.19	42.29 ± 1.50
AHM75	33.12 ± 0.52	75.00 ± 0.89	62.15 ± 0.44	65.90 ± 1.08	78.18 ± 0.62	80.34 ± 1.84	46.20 ± 0.82	83.20 ± 1.58	50.13 ± 1.62
AHM80	70.54 ± 1.05	58.22 ± 0.66	50.27 ± 0.36	74.33 ± 1.33	60.13 ± 0.45	78.00 ± 1.90	71.00 ± 1.20	90.16 ± 1.65	39.42 ± 1.40
AHM85	50.18 ± 0.71	44.62 ± 0.50	23.94 ± 0.09	50.88 ± 0.87	80.11 ± 0.70	52.95 ± 1.30	30.70 ± 0.60	44.05 ± 0.78	70.11 ± 1.99
AHM90	28.55 ± 0.47	77.50 ± 0.89	80.00 ± 0.72	53.26 ± 0.92	64.92 ± 0.55	71.18 ± 1.68	61.99 ± 1.00	38.90 ± 0.65	50.92 ± 1.68
AHM96	59.21 ± 0.79	50.76 ± 0.61	63.35 ± 0.50	76.27 ± 1.00	90.93 ± 0.86	95.19 ± 2.23	86.15 ± 1.33	91.26 ± 1.60	79.42 ± 2.15
AHM100	22.17 ± 0.38	43.18 ± 0.51	55.29 ± 0.41	59.40 ± 0.88	44.10 ± 0.30	38.11 ± 0.79	50.10 ± 0.91	60.04 ± 0.91	20.93 ± 0.72
AHM105	34.00 ± 0.51	60.35 ± 0.68	74.35 ± 0.63	70.23 ± 1.16	81.75 ± 0.69	80.19 ± 1.77	67.15 ± 1.20	71.31 ± 0.98	65.20 ± 1.94
AHM110	65.29 ± 0.96	50.29 ± 0.59	58.00 ± 0.42	49.50 ± 0.82	70.36 ± 0.63	67.50 ± 1.60	70.20 ± 0.25	88.51 ± 1.50	19.56 ± 0.75
AHM115	49.77 ± 0.56	31.50 ± 0.38	40.32 ± 0.30	58.16 ± 0.80	80.20 ± 0.72	48.37 ± 0.85	81.10 ± 1.40	90.18 ± 1.58	71.26 ± 1.98
AHM120	41.20 ± 0.64	59.10 ± 0.72	50.15 ± 0.39	39.83 ± 0.63	67.19 ± 0.55	70.00 ± 1.52	40.25 ± 0.79	52.00 ± 0.84	68.83 ± 1.84
AHM125	18.19 ± 0.32	66.13 ± 0.79	61.40 ± 0.46	55.18 ± 0.96	86.00 ± 0.74	82.62 ± 1.90	60.18 ± 0.98	76.20 ± 1.14	25.48 ± 0.86
AHM130	50.14 ± 0.66	74.21 ± 0.84	59.83 ± 0.50	62.50 ± 1.02	88.16 ± 0.93	32.77 ± 0.72	27.19 ± 0.48	70.25 ± 0.99	69.52 ± 1.79
AHM135	78.00 ± 1.12	40.50 ± 0.51	30.81 ± 0.19	73.32 ± 1.21	60.02 ± 0.49	30.15 ± 0.66	51.66 ± 0.83	90.00 ± 1.47	43.66 ± 1.40
AHM140	39.54 ± 0.37	73.00 ± 0.81	63.10 ± 0.50	51.29 ± 0.79	78.00 ± 0.72	88.45 ± 2.13	66.82 ± 1.32	50.16 ± 0.81	64.24 ± 1.78

Averages are from triplicate experiments. Initial PAHs concentrations were 500 mg/L.

isolated from the mycobiome of these effluents against heavy metals, hydrocarbons and other pollutants from real petroleum effluents and aqueous solutions and selection of the hyperactive strains, (3) Improving the iron and cobalt removal and absorption coefficients, which were detected in the highest toxic amounts in all refineries effluents. These parameters include the nature of biomass (metabolic or non-metabolic), temperature, initial pH, initial concentration of each heavy metals, biomass doses, operating time in batch mode, (4) comprehensive analysis of the uptake of metal ions into the fungal biomass by applying SEM-EDX and FTIR spectroscopy as well as (5) evaluation of the removal of heavy metals and other pollutants from the wastewater of Mostorod, Ameria and Tanta refineries under optimal conditions.

2. Materials and methods

2.1. Chemicals, media and petroleum refining effluents

Acenaphthylene, anthracene, acenaphthene, Benz[a]anthracene, phenanthrene, fluoranthene, Benzo[a]pyrene, chrysene and pyrene of high-purity grade were purchased from Sigma Chemical Company. Solvents were in analytical grade (Merck Laboratory Supplies). Fungal cultivation media and their components were obtained from Difco Laboratories. Refinery effluents were collected from three different refining areas in Egypt including Mostorod (the north of Capital Cairo), Ameria (the west north of Alexandria) and Tanta (Delta region) refineries at a discharge point, transported to laboratory in ice tank and preserved at 4 °C until analysis.

2.2. Analysis of petroleum refining wastewater

Parameters and analytical methods of all collected samples include chemical oxygen demand (COD), total suspended solids (TSS), total dissolved solids (TDS), biological oxygen demand (BOD_5), cations, anions, BTX (Benzene, toluene, xylene), phenols, polycyclic aromatic hydrocarbons (PAHs), total petroleum hydrocarbons (TPH), oil and grease, total nitrogen, electrical conductivity (EC), total phosphorus, pH, turbidity and coloration degree were examined according to the standard methods for examination of water and wastewater (American Public Health Association, APHA, 1995; 1998, 2012, 2018), and the method described by Zhang et al. (2009), Yue et al. (2016) and Zhang et al. (2018).

2.3. Preparation of heavy metals concentrations

Standard heavy metal solutions and the freshly diluted solutions were prepared by deionized water. These assessments were executed by Atomic Absorption Spectrophotometer and the pH of each metal ion solution was amended to the required values by either concentrated nitric acid (65%) or sodium hydroxide (1 M) (Biswal and Agrawal, 2016).

2.4. Isolation of the indigenous fungal strains

Fungal biosorbents were isolasted from the petroleum refining wastewater collected from water drainage areas of Mostorod (MRWW), Ameria (ARWW) and Tanta (TRWW) refineries, individually by the serial dilution technique using mineral salt agar medium (MSA) composed of (g/L; NaCl 0.5, $NaNO_3$ 0.2, $MgSO_4.7H_2O$ 0.025, K_2HPO_4 0.5, KH_2PO_4 0.5), and supplemented with 1% crude oil at pH 5.5. Plates were incubated at 30 °C for 2 weeks in dark and examined daily for the appearance of fungal growth. Single pure fungal colonies were inoculated into the potato dextrose agar medium, incubated for 5 days at 30 °C and then preserved at 4 °C for further studies.

2.5. Screening and evaluation of the bioremoval efficiency of metal ions and other pollutants from the refineries wastewater by the live biomass of the oily effluents mycobiome

The biosorption tests were carried out in 500 mL flasks containing 0.4% biosorbent dosage (live biomass) of one of the fungal sorbents under study in 300 mL wastewater mixture of MRWW, ARWW and

TRWW (1: 1: 1) at 40 °C and pH 5.5 for 120 min as a contact time on a rotary shaker (120 rpm). After that, the samples were centrifuged at 10,000 rpm for 15 min and then physicochemical parameters were determined in the refining wastewater after bioremediation treatments with the twenty fungal isolates individually. Wastewater without adding biomass served as a control. Trials were done in triplicate and average values were calculated. To estimate bioremoval efficiency percentage (RE%) for each heavy metal or parameter from refinery effluents or aqueous solutions by each isolate, the following equation was applied:

$$\text{Biosorption\% (R\%)} = (\text{Ci} - \text{Cf}) / \text{Ci} \times 100 \quad (1)$$

Where Ci, is the initial parameter concentration and Cf, is the residual concentration (mg/L) in the solution was applied. The atomic absorption spectroscopy (AAS) technique was used for determining the concentration of heavy metals by using the specific lamb at the specific wavelength for each metal ion (El-Gendy et al., 2011, 2017; Aishwarya et al., 2017).

2.6. Adsorption of polycyclic aromatic hydrocarbons (PAHs) from aqueous solution by the live biomass of the oily effluents mycobiome

Experiments were conducted on the nine PAHs individually. The analysis of PAHs adsorption capacity of each fungal strain as adsorbent against phenanthrene, acenaphthylene, fluoranthene, acenaphthene, anthracene, pyrene, benz[*a*]anthracene, chrysene and Benzo[*a*]pyrene, individually from aqueous solution was done in batch equilibrium adsorption experiments using UV–VIS spectrophotometry (SHIMADZU UV-1700) as described by Brandão et al. (2010) and Puszkarewicz and Kaleta (2020). Experiments were performed in flasks contains 500 mg/L hydrocarbon, fungal biomass dosage of 4 mg/L in 100 mL acetonitrile-water solution agitated in a shaker at 120 rpm for 24 h at 30 °C. Control samples without fungal biomass were included. Each hydrocarbon concentration after adsorption treatment by each fungal biomass was determined. The amounts of hydrocarbon adsorption qe (mg/g) were calculated by the equation:

$$qe=(C_0–C_e).\ V / M \quad (2)$$

Where C_0 is initial concentration of hydrocarbon (mg/L), Ce is residual concentration of hydrocarbon (mg/L), V is the volume of solution (L) and M is mass of adsorbent (g). Percentage adsorption was calculated using equation:

$$\text{Percentage adsorption (\%)} = (C_0–C_e) / C_0 \times 100 \quad (3)$$

The experiments were triplicated and the average values were taken for data analysis.

2.7. Morphological and biochemical identification of the hyperactive biosorbent isolates AHM69 and AHM96

Analysis of the fatty acid profile was achieved by GC/MS analysis with Agilent 6890N Gas Chromatograph associated to Agilent 5973 Mass Spectrometer at 70 eV. The carrier gas helium was conserved at a flow rate of 1.0 mL/min. The inlet temperature was conserved at 300 °C, and the oven was programmed for 2 min at 150 °C, then increased to 300 °C at 4 °C/min and maintained for 20 min at 300 °C. The injection volume was 1 mL, with a split ratio of 50:1. Structural assignments were based interpretation of mass spectrometric fragmentation and established by compare of retention time, fragmentation pattern of authentic compounds and the spectral data acquired from Wiley and NIST libraries. Furthermore, macro-morphological (color, texture, appearance and diameter of the colonies) and micro-morphological (spores, sporophores and mycelium shape) properties were characterized. Both of phenotypic and chemotypic were achieved as previously described (Larone, 1995; Silva et al., 1998; Samson et al., 2007; Fraga et al., 2008; Tiwari et al., 2011; Zain et al., 2013; Kidd et al., 2016).

Table 4. Phenotypic and chemotypic characteristics of the selected fungal isolates AHM69 and AHM96.

Characteristics	Percentage of total fatty acid content (%)	
	AHM69	AHM96
Caprylic acid (octanoate C8:0)	0.02 ± 0.10	N.D
Lauric acid (dodecanoic acid C12:0)	0.01 ± 0.10	N.D
Myristic acid (C14:0)	0.49 ± 0.76	0.58 ± 0.45
Pentadecanoic (15:0)	N.D	8.03 ± 0.50
Palmitic acid (C16:0)	31.38 ± 0.78	11.87 ± 0.59
Palmitoleic acid (C16:1)	0.38 ± 0.38	1.29 ± 0.31
Margaric acid (C17:0)	0.19 ± 0.32	1.57 ± 0.10
Margaroleic acid (C17:1, w8)	N.D	0.77 ± 0.19
Stearic acid (C18:0)	10.41 ± 1.09	16.33 ± 0.81
Oleic acid (C18:1)	19.67 ± 0.34	20.10 ± 0.54
Linoleic acid (C18:2)	24.70 ± 4.30	39.63 ± 1.09
Linolenic acid (C18:3)	11.94 ± 0.16	N.D
Arachidic acid (C20:0)	0.48 ± 0.16	0.49 ± 0.06
Eicosenoic acid (C20:1)	N.D	0.34 ± 0.74
Eicosadienoic acid (C20:2)	N.D	0.34 ± 0.09
Behenic acid (C22:0)	0.33 ± 0.76	N.D
Phenotypic characteristics	On Czapek's agar (CZ), colonies were irregular, compact, greyish green with a suede-like surface covered by a dense of conidiophores with layer of dark-brown to black large globose and biseriate conidial heads (4–6 mm × 16–22 μm in diameter). Reverse was whitish yellow to beige. Older conidial heads become radiate and tend to divided into a number of loose columns. Conidiophore was smooth-walled, short, hyaline with club-shaped terminal vesicles which were uni-seriate and support phialides on the upper two thirds of the vesicle. Conidia are globose to subglobose (4.5–6.5 μm in diameter), dark brown to black and roughened-walled.	On Czapek's agar (CZ), colonies were circular, concave in centers, texture velvety, blue-green surface but reverse yellowish brown with buff centers. Sporulation very dense. Soluble pigments and exudates are absent. Conidiophores are hyaline, biverticillate, supporting phialides in brush-like clusters, stipes septate, smooth-walled and 100–135×4–6 μm in diameter. 5–8 Phialides from branched cylindrical metulae (10.5–15.0 × 3.5–4.5μm) were formed at the ends of the conidiophores. Phialides are flask-shaped, composed of a cylindrical basal part and a distinct neck, 9.0–12.0 × 3.3–4μm. Conidia are dull green, ellipsoidal, smooth-walled in long dry chains.

2.8. Molecular identification of promising fungal biosorbents

The extraction and purification of fungal genomic DNA was performed by a QIAGEN DNeasy Tissue Kit (El-Bondkly, 2012; El-Gendy et al., 2018). Specific fungal PCR performed by puReTaq™Ready-To-Go™ PCR Beads with the primers of ITS1 (5′-TCC GTA GGT GAA CCT GCG G-3′) and ITS4 (5′-TCC TCC GCT TAT TGA TAT GC-3′). PCR amplification performed according to White et al. (1990), El-Bondkly (2012) and

El-Gendy et al. (2018). PCR products tested to determine their correct length and then PCR products were purified and sequenced (White et al., 1990). Sequence data were edited with Lasergene SeqMan (DNAStar Inc.). Next, relatives were identified compared to rRNA genes in the National Center for Biotechnology Information (NCBI) GenBank database by Basic Local Alignment Search Tool (BLAST; http://www.ncbi.nlm.nih.gov website) to construct a matrix using MEGA-X. The topology of the trees was evaluated through bootstrap analysis based on 1000 replicas using MEGA-X and the phylogenetic tree was derived by the neighbor-joining method (Tamura et al., 2011; Kumar et al., 2018).

2.9. Preparation of the dead and live biomasses of the selected fungal isolates AHM69 and AHM96

Spores from each fungal isolate (10^6 CFU/mL), AHM69 and AHM96, individually were moved into 500 mL Erlenmeyer flasks containing 100 mL liquid medium g/L; yeast extract 5, malt extract 10, peptone 5, and glucose 20 in distilled deionized water and incubated at 30 °C for 10 days in dark. The resulting biomass of each fungal isolate was filtrated through Whatman No. 1, washed many times with 0.1 M NaCl and distilled water to eliminate non biomass particles. Dead biomasses of these fungi were achieved through autoclaving a portion of each biomass at 121 °C for 15 min while another portion serves as live biomass. Both autoclaved and non-autoclaved biomasses were dried, powdered by a mortar and applied as dead and live fungal biomasses for bio-removal studies (El-Gendy et al., 2011; El-Gendy and El-Bondkly, 2016).

2.10. Optimization of the operational factors affecting the removal of Fe^{3+} and Co^{2+} from the aqueous solution by biomass AHM69 and AHM96 strains

The biosorption tests were carried out in flasks having 0.4% biosorbent dosage (AHM69 and AHM96, individually) in 100 mL metal solution including 200 mg/L of each of the selected heavy metal under study Fe^{3+} and Co^{2+} on a rotary shaker at 120 rpm, 40 °C, pH 5.5 and 120 min as a contact time. The biosorption operational parameters were optimized using different temperatures (25, 30, 35, 40, 45, 50, 55, 60, 65 and 70 °C) and pH (3.0, 4.0, 4.5, 5.0, 5.5, 6.0, 7.0, 8.0, 9.0 and 10.0) using 0.4% biosorbent dosage of both live and dead forms of the selected fungal biomass, individually. The effect of different initial metals concentration (50, 100, 200, 300, 400 and 500 mg/L of both metals) at different contact times (10 min–1440 min) as well as various live biosorbent dosages (0.05, 0.1, 0.2, 0.3, 0.4, 0.5 and 1.0%) of AHM69 and AHM96, separately at higher metal concentrations i.e., 400, 500 and 1000 mg/L of Fe^{3+} and Co^{2+} heavy metals for 180 min as contact time on the validity of bioremediation were evaluated. The parameter being optimized was applied in the next experiment and so on until the optimization process is completed based on the previous reports (El-Gendy et al., 2011, 2017; Alzahrani et al., 2017; Alzahrani and El-Gendy, 2019).

2.11. Removal of heavy metals and other contaminants from petroleum refining wastewater under optimized conditions

The adsorption experimental procedure was performed on the three wastewater samples collected from different petroleum refining areas in Egypt including (Mostorod in Cairo, America in Alexandria and Tanta in Delta) using the selected fungal strains under the optimized conditions at the optimum pH, temperature and contact time that was determined from the previous optimization experiments. The percentage of removal after the sorption experiment was detected as mentioned above.

2.12. Fourier transform infrared spectroscopy (FT- IR) analysis

FT-IR was applied for define vibration frequency groups in the biosorbents after as well as before treatment with Fe^{3+} and Co^{2+}. For the IR experiments, the dried fungal biomasses before and after bioremoval studies were blended with KBr and grounded in an agate mortar. The combination squeezed to form pellets and apply in spectral recording by the Broker Vertex80v (Germany) in the range of 4000–400 cm^{-1} with resolution 4 cm^{-1} at the central laboratory of National Research Centre, Egypt. Characteristics and identification of peaks in this investigation were based on known results from the previous literatures.

2.13. Scanning electron microscope (SEM) analysis and energy-dispersive X-ray spectroscopy (EDX) analysis

Effects of both heavy metal ions Fe^{3+} and Co^{2+} on the fungal surface morphology were examined by SEM. The fungal biomass amended with a mixture of Fe^{3+} and Co^{2+} at initial concentration of 500 mg/L were used for SEM analysis along with control using a high resolution scanning electron microscopy (SEM Quanta FEG 250 with field emission gun, FEI Company – Netherlands) at the Central Laboratory (National Research Centre, Egypt). To enhance the quality and increase the electron conduction of the microscopic images, both untreated and metal-absorbed fungal biomass were mounted on a stainless steel with a coating of thin layer of gold under vacuum. Confirmation of presence of metal ions on the fungal biomass surface was tested using EDX analysis using an X-ray micro-analyzer connected to a scanning electron microscope. The individual ratios given represent the average of ten measurements. It should be noted that SEM-EDX measures the percentage of detected elements with respect to each other so that the sum of percentages of all detected elements is 100.

2.14. Statistical analysis

The results were statistically processed by analyzes of variance (ANOVA), followed by T- or Tukey's tests when significant effects were detected ($P \leq 0.05$). Data were expressed as means ± standard error.

3. Results and discussion

3.1. Physicochemical analysis of the petroleum refining wastewater at different locations in Egypt

According to Decree of Health Ministry (No. 458, 2007), WHO (2011), Ayers and Westcot (FAO 1994), American Public Health Association (APHA 1998, 2012) and Canadian Council of Ministers of the Environment (CCME 1999, 2007, 2011, 2014) criteria, all petroleum refining effluents under consideration contain much higher amounts of pollutants and are classified as highly polluted with heavy metals (Table 1). Moreover, the composition and amount of each pollutant of such refinery wastewater was varying depending upon the operational units and locations at Cairo, Alexandria or Tanta (Table 1). Data in Table 1 give the abundance of the cations in the following order; Na^+ (from 3000.39 ± 8.05 to 4160.73 ± 8.75 mg/L) > Fe^{3+} (from 3085.45 ± 6.20 to 3452.41 ± 5.91 mg/L) > Ca^{2+} (from 480.13 ± 1.92 to 554.20 ± 2.07 mg/L) > Mg^{2+} (from 320.15 ± 1.20 to 370.8 ± 1.50 mg/L) > Co^{2+} (from 289.74 ± 0.58 to 300.20 ± 0.75 mg/L) > Mn^{2+} (from 281.40 ± 0.89 to 290.51 ± 0.91 mg/L) > Ba^{2+} (from 145.59 ± 1.53 to 195.80 ± 1.73 mg/L) > Al^{3+} (from 134.40 ± 1.26 to 196.01 ± 1.17 mg/L) > K^+ (from 129.28 ± 3.40 to 140.18 ± 3.06 mg/L) > B^+ (from 68.42 ± 0.34 to 90.16 ± 0.45 mg/L) > Zn^{2+} (from 30.16 ± 0.26 to 40.23 ± 0.29 mg/L) > Pb^{2+} (from 25.89 ± 0.36 to 28.3 ± 0.31 mg/L) > Ni^{2+} (from 20.50 ± 0.21 to 24.89 ± 0.24 mg/L) > Cu^{2+} (from 16.89 ± 0.25 to 22.87 ± 0.21 mg/L) > As^{3+} (from 6.20 ± 0.10 to 9.60 ± 0.15 mg/L) > Cr^{6+} (from 5.83 ± 0.08 to 9.18 ± 0.11 mg/L) > Cd^{2+} (from 2.20 ± 0.05 to 3.73 ± 0.09 mg/L) > Ag^+ (from 2.19 ± 0.05 to 3.15 ± 0.12 mg/L) > Hg^{2+} (from 0.049 ± 0.003 to 0.061 ± 0. 005 mg/L).

These results clearly indicated that both iron and cobalt recorded the highest concentrations among all heavy metals in the wastewater of all petroleum refineries. According to the internationally permissible ratios, the detected concentrations of Fe^{3+} and Co^{2+} are highly toxic to all forms

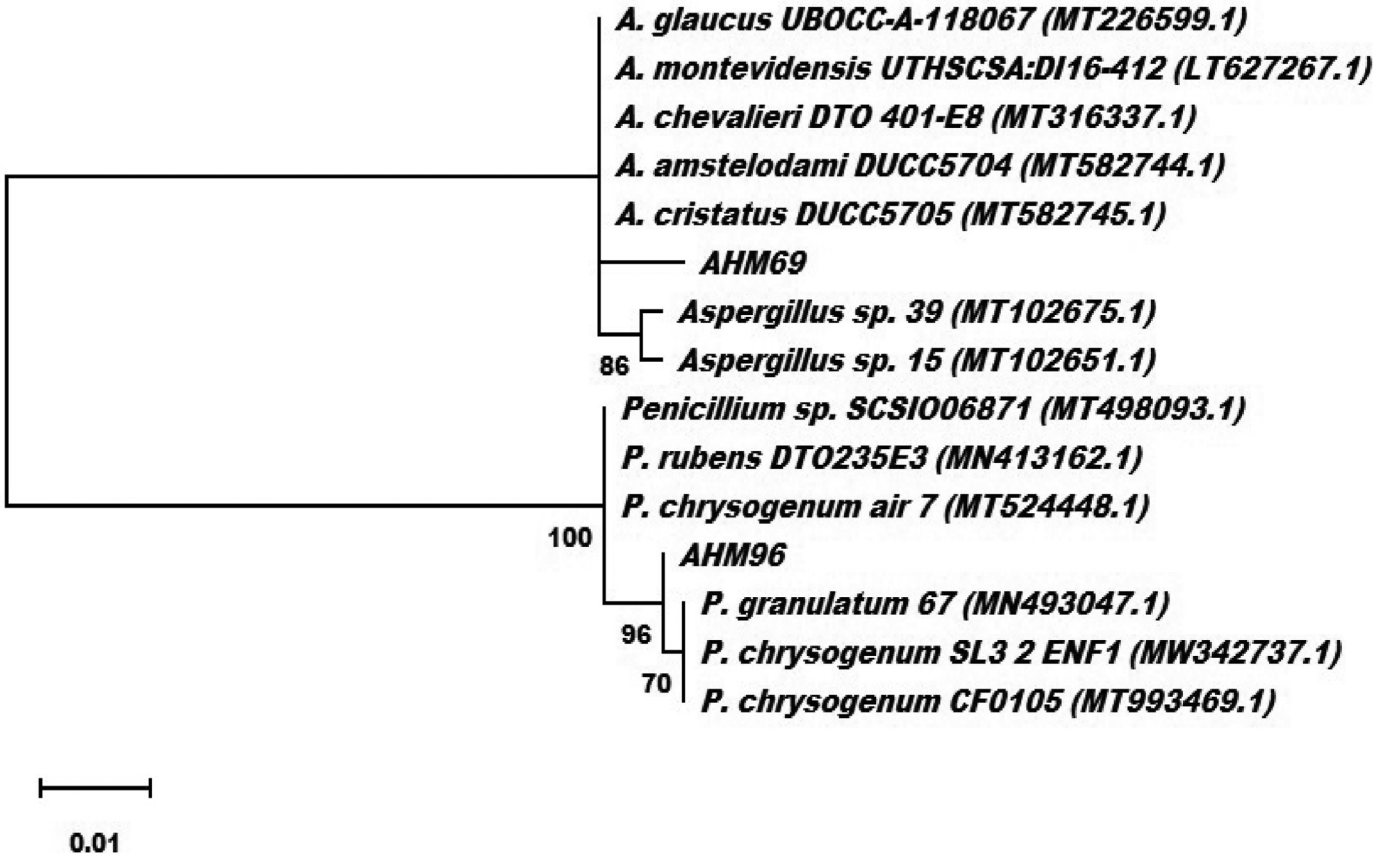

Figure 1. Phylogenetic tree of selected fungal strains AHM69 and AHM96 based on rDNA-ITS sequences analysis.

of life, in addition to the fact that previous reports their biological removal from industrial wastewater are very scarce, and therefore these two heavy metals were selected for optimization studies by the hyper active fungal biosorbents. Universally, the heavy metals responsible for environmental contamination are cadmium (Cd^{2+}), cobalt (Co^{2+}), chromium (Cr^{6+}), zinc (Zn^{2+}), nickel (Ni^{2+}), copper (Cu^{2+}), lead (Pb^{2+}), Iron (Fe^{3+}) and mercury (Hg^{2+}), which are generated from different sources and industries as refinery, metal finishing, electroplating,

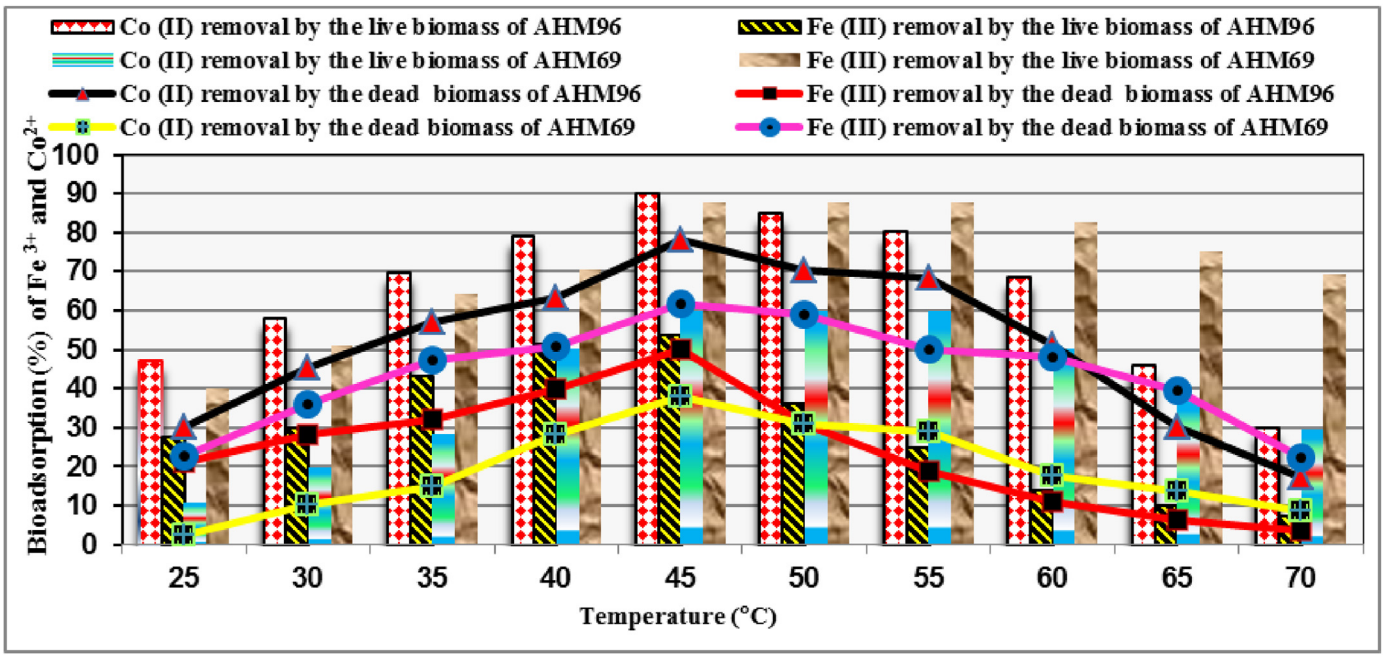

Figure 2. Effect of various process temperatures on the bioremoval of Fe^{3+} and Co^{2+} (%) from aqueous solution by live and dead biomasses of *Aspergillus* sp. AHM69 and *Penicillium* sp. AHM96.

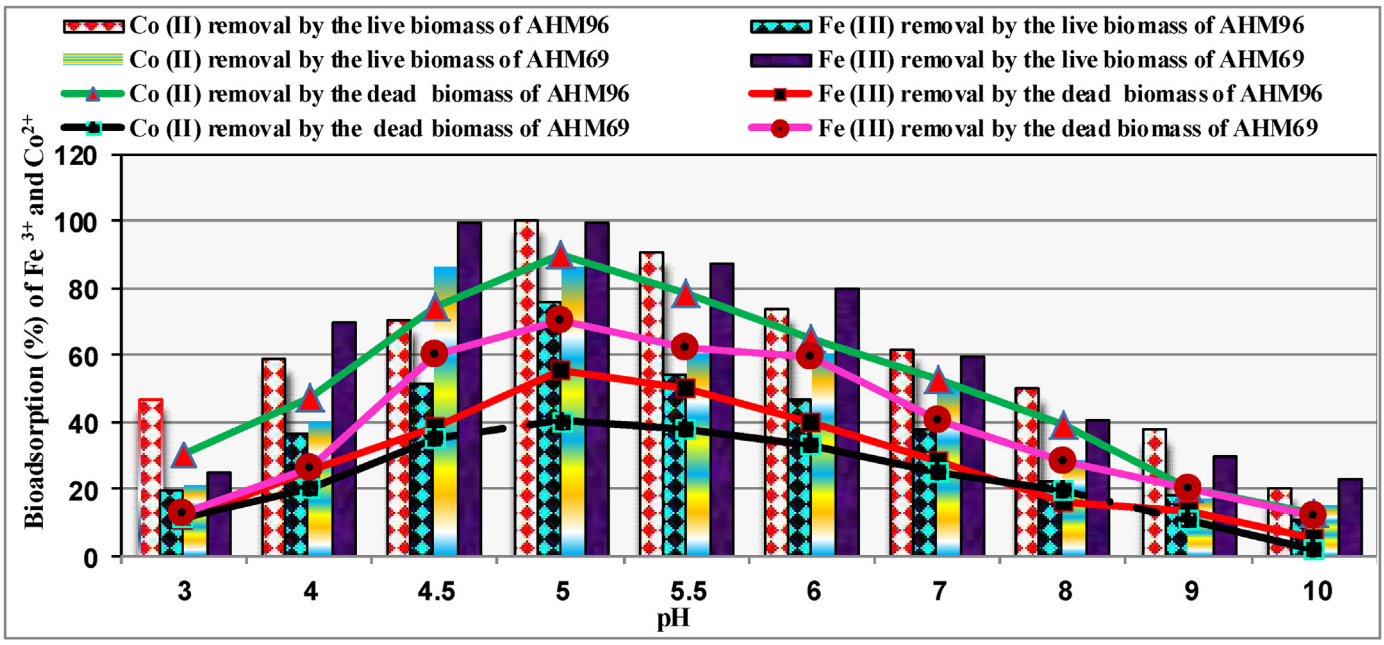

Figure 3. Effect of various pHs on the biosorption process of Fe^{3+} and Co^{2+} (%) from aqueous solution by live and dead biomasses of *Aspergillus* sp. AHM69 and *Penicillium* sp. AHM96.

tanning, chemical manufacturing, fertilizer and mining (Dusengemungu et al., 2020). Moreover high values of total dissolved solids (TDS; from 4095.39 ± 20.84 to 4240.61 ± 20.20 mg/L), chemical oxygen demand (COD; from 2520.34 ± 23.27 to 3150.00 ± 24.15 mg/L), oil and grease (from 1643.00 ± 5.83 to 1690.87 ± 5.60 mg/L), biochemical oxygen demand (BOD_5; from 1081.12 ± 3.39 to 1382.58 ± 3.44 mg/L), total suspended solids (TSS; from 750.62 ± 4.46 to 800.14 ± 5.12 mg/L), benzene, toluene, xylene (BTX; from 150.60 ± 2.13 to 179.50 ± 1.95 mg/L) and phenols (from 19.23 ± 2.21 to 22.11 ± 2.54 mg/L) were recorded (Table 1). Furthermore anions were determined to be Cl^- (from 6310 ± 19.12 to 8227 ± 18.20 mg/L), SO_4^{2-} (from 70.13 ± 1.90 to 92.61 ± 1.10 mg/L), NH_3–N (from 71.00 ± 2.19 to 80.25 ± 2.70 mg/L), NO_3–N (from 5.83 ± 0.80 to 6.18 ± 0.74 mg/L) and phosphorus (PO_4; from 2.14 ± 0.90 to 3.50 ± 0.88 mg/L) (Table 1). In addition, EC (from 19,237 ± 26.70 to 24,120 ± 30.69 μs/cm), turbidity (from 400 ± 7.70 to 419 ± 7.95 NTU) and color (from 5409 ± 20.04 to 5655 ± 19.54 Pt Co) were detected in these refineries wastewaters under study (Table 1). It is believing that refining and petrochemical industrial wastewater are the most difficult to treat due to the high organics load, a wide range of hydrocarbon species and lots of free oil, very high COD to BOD ratios, along with there are many recalcitrant and inhibitory compounds in the wastewater influent (Wei et al., 2020). Ishak and Malakahmad (2013) reported that petroleum refinery wastewater characteristics were COD, BOD_5, nitrate, TSS, ammonia nitrogen, oil and grease, phosphorus, TOC, phenols, sulphate, benzene, toluene, ethylbenzene and xylene (1673, 448, 4.90, 310, 45, 97, 1.70, 1217, 1.44, 50, 33.85, 39.83, 1.85, and 30.03–33.04 mg/L) as well as turbidity (419 NTU), and color (3650 Pt Co), which are lesser than the results of the current study. On the other hand, much higher amounts were reported by Dincer et al. (2008) for COD, BOD, TSS, ammonia, oil and grease and TDS (21000, 8000, 2580, 69, 1140, and 37000 mg/L) in the refinery wastewater. Interestingly, as presented in Table 1, the pH of all petroleum refining wastewater under study was highly acidic and ranged from pH from 2.5 ± 0.02 to 2.8 ± 0.02 which is far above the legal requirements and promotes the dissolution of toxic metals. In line with our data Dincer et al. (2008) note that the pH of petroleum wastewater is equal to 2.50 which can be described as highly acidic. The acidity of these petroleum effluents may be attributed to their higher contents of metals are hydrolysed and then lowers the pH of the water and soil making it unsuitable and causing dangerous effects on terrestrial and aquatic organisms, hence the petroleum

Table 5. Effect of different initial heavy metals concentrations on the efficiency of bioremoval process by live biomass of *Aspergillus* sp. AHM69 at various contact times.

Time (min)	Concentration of heavy metal (mg/L)											
	50		100		200		300		400		500	
	Removal (%)											
	Fe^{3+}	Co^{2+}	Fe^{3+}	Co^{2+}	Fe^{3+}	Co^{2+}	Fe^{3+}	Co^{2+}	Fe^{3+}	Co^{2+}	Fe^{3+}	Co^{2+}
10	100.0	60.13	88.25	44.60	61.10	40.30	65.20	30.70	58.32	20.41	40.03	13.78
30	100.0	76.45	100.0	57.35	90.00	51.66	81.38	42.52	70.49	31.00	58.40	25.50
60	100.0	89.58	100.0	72.20	100.0	68.92	100.0	59.13	88.61	46.18	70.81	39.24
120	100.0	100.0	100.0	86.95	100.0	83.50	100.0	70.32	100.0	58.33	93.10	50.74
180	100.0	100.0	100.0	100.0	100.0	95.63	100.0	91.15	100.0	86.19	100.0	73.11
240	100.0	100.0	100.0	100.0	100.0	99.21	100.0	90.68	100.0	80.71	100.0	66.23
300	100.0	100.0	100.0	100.0	100.0	100.0	100.0	90.21	100.0	80.50	100.0	60.51
360	100.0	100.0	100.0	90.17	100.0	84.22	100.0	75.10	100.0	72.50	100.0	53.23
420	100.0	98.28	100.0	84.55	100.0	70.16	100.0	62.35	100.0	59.06	100.0	40.35
1440	100.0	90.00	100.0	76.42	100.0	63.14	100.0	50.21	100.0	30.00	100.0	23.14

industries and refineries wastewater need treatments chemical, physical or biological (Varjani et al., 2020).

3.2. Evaluation of different fungal isolates as biosorbents for metal ions removal from petroleum refining wastewater

In the current work, 20 fungal isolates were isolated from different three petroleum refining wastewater. These isolates were under the isolation codes AHM50, AHM55, AHM60, AHM65, AHM69 and AHM70 that isolated from Mostord refining effluent and AHM75, AHM80, AHM85 and AHM90 isolated from Amerya refining effluent while AHM96, AHM100, AHM105, AHM110, AHM115, AHM120, AHM125, AHM130, AHM135 and AHM140 were isolated from Tanta refining effluent. The results in Table 2 show that the live biomass of the fungal isolates individually was found to remove appreciable amounts of heavy metals and other pollutants from individual refinery effluents. Among them, the AHM69 biomass supported the highest removal efficiency (RE = 100%) of Al^{3+}, Fe^{3+}, Mn^{2+}, Zn^{2+}, Pb^{2+}, Ni^{2+} and As^{3+} followed by Cu^{2+}, Na^{+}, Ca^{2+}, Cr^{6+} and Cd^{2+} (RE = 97.10 ± 0.66, 90.85 ± 0.85, 90.66 ± 0.50, 84.54 ± 0.60 and 75.83 ± 0.90%, respectively) for 120 min as contact time. However, it was observed that the binding sites in AHM96 biomass showed the highest removal efficiency (RE = 100%) for Zn^{2+}, Pb^{2+}, Co^{2+}, Cd^{2+} and Cr^{6+} subsequent by Al^{3+}, Mn^{2+}, As^{3+}, Cu^{2+}, Na^{+}, Ca^{2+} and Ni^{2+} (RE = 94.22 ± 0.61, 90.0 ± 0.29, 90.0 ± 0.26, 89.81 ± 0.70, 84.32 ± 1.1, 84.30 ± 0.32 and 82.59 ± 0.90%, respectively), for 120 min as contact time (Table 2). This behavior of both strains can be demonstrated by their superior capability to sequester substantial amounts of the metals from aqueous solution compared to other isolates. Fungi have certain advantages over bacteria with regard to bioadsorption and biodegradation because of their resistance to heavy metals and acidic pH that found in refinery wastewater. For example, *Aspergillus* sp., *Rhizopus* sp., *Aspergillus fumigatus*, *Irpex lacteus* and *Pleurotus ostreatus* show exceptional bioadsorption ability against petroleum toxicants including heavy metals from a contaminated environment by the petroleum industries and refineries wastewater (Al-Hawash et al., 2019). Whereas iron and cobalt in low concentrations are necessary for certain biochemical and physiological activities in the body, the exposure of living organisms to high concentration of iron and cobalt have adverse health effects that include generation of free radicals to cause oxidative stress and damage to biological molecules as enzymes, proteins, lipids and DNA which are key to carcinogenesis and may damage many organs of the body such as the brain, lungs, liver and kidney. In addition, they cause nausea, diarrhea, blood disorders, miscarriages, reproductive disorders, dermatitis, internal haemorrhage, respiratory problems and a significant increase in the risk of lung, bladder, skin, liver cancers (Engwa et al., 2019)

Furthermore, potent reduction efficiency in BOD (RE = 98.0 ± 0.55 and 94.91 ± 0.50%), TOC (RE = 90.80 ± 1.14 and 85.06 ± 0.39%), COD (RE = 97.25 ± 0.80 and 95.80 ± 0.35%), TSS (RE = 99.20 ± 0.53 and 98.0 ± 0.22%), TDS (RE = 95.12 ± 0.60 and 96.40 ± 0.72%), turbidity (RE = 87.31 ± 0.60 and 89.0 ± 0.69%), total nitrogen (RE = 92.50 ± 0.46 and 94.4 ± 0.59%), total phosphorus (RE = 90.20 ± 0.70 and 88.21 ± 0.51%) were achieved after treatment of the refinery wastewater with the live biomass of AHM69 and AHM96, respectively (Table 2). Interestingly both strains were able to reduce petroleum hydrocarbons and oily pollutants including PAHs (RE = 99.91 ± 1.16 and 98.26 ± 0.86%), TPHs (RE = 98.15 ± 1.22 and 99.20 ± 0.91%), BTX (RE = 90.31 ± 0.42 and 85.76 ± 0.31%), phenols (RE = 97.0 ± 0.90 and 90.11 ± 1.02%), oil and grease (RE = 98.15 ± 1.12 and 99.10 ± 0.96%) after treatment with the live biomass of AHM69 and AHM96, respectively (Table 2), Samanta and Mitra (2021) reported that the earth's surface water and ground water affected by the contaminated wastewater from petroleum industries, thereby their toxic components including organic and inorganic components need to be well managed before discharging to any receiving waters by indigenous fungi that have been well developed for organic and inorganic wastewater treatment are thus a potential process for petrochemical wastewater management (Mawad et al., 2020).

3.3. Evaluation of the bioremovval capacity of polycyclic aromatic hydrocarbons (PAHs) by the live fungal biomasses as adsorbents from aqueous solutions

Adsorption capacity of each fungal biomass against different PAHs include anthracene, acenaphthylene, phenanthrene phenanthrene, acenaphthene, fluoranthene, pyrene, benz[a] anthracene, chrysene and benzo[a] pyrene, individually are displayed in Table 3. As is clearly evident from the removal efficiency (RE%) results in Table 3 the biomass of AHM69 was most efficient for the bioremoval of low molecular weight PAHs that characterized by three benzene rings including acenaphthylene, acenaphthene, phenanthrene and anthracene (83.55 ± 1.24, 80.90 ± 0.95, 84.31 ± 0.69 and 90.25 ± 1.34%, respectively) (Table 3). However, the strain AHM96 showed the highest reduction activity (RE) in the descending order, toward the higher molecular-weight PAHs with four benzene rings fluoranthene, chrysene, benz[a]anthracene and benzo [a]pyrene with five benzene rings (RE = 90.93 ± 0.86, 91.26 ± 1.60, 86.15 ± 1.33, and 79.42 ± 2.15%, respectively) (Table 3). Over the past decades, a large amount of PAHs has been released into the environment as a result of various petrochemical-related activities that can pose a significant risk to human health and the environment but the use of fungal biomass-derived adsorbents belong to the *Penicillium*, *Aspergillus*, *Fusarium*, *Trichoderma*, *Pleurotus*, *Cladosporium*, *Phanerochaete*, *Candida* and *Monicillium* genera has received much consideration across the environmental field as an effective method for PAHs and other petroleum pollutants removal from water as a promising environmentally-friendly and low-cost option (Sharma et al., 2022; Simarro et al., 2013; Vahabisani and An, 2021). Consequently, the fungal strains AHM96 and AHM69, which showed the highest bioremoval activity against heavy meals Fe^{3+} and Co^{2+}, respectively and other pollutants in the refineries effluent as well as the hyper adsorption efficiently toward PAHs from aqueous solutions, then they were selected as biosorbents for more studies.

3.4. Identification of the selected isolates AHM69 and AHM96

The selected isolates were initially determined based on their morphological and biochemical properties followed by phylogenetic analysis of their ITS1 and ITS4 sites of rDNA. Morphological properties demonstrated that the AHM69 fungal strain belonged to *Aspergillus* species; it was grow rapidly to form cottony colonies on Czapek's agar (CZ) at 28 °C. The colonies were irregular, compact grayish green with a suede-like surface covered by a dense of conidiophores with layer of dark-brown to black large globose and biseriate conidial heads (4–6 mm × 16–22 μm in diameter) while reverse was whitish yellow (Table 4). With the maturation of the colony, the color of the reverse side changed from whitish yellow to beige, obverse became dark greenish gray and older conidial heads become radiate and tend to divided into a number of loose columns. The conidiophore is short, hyaline, smooth-walled, and had club shaped terminal vesicles that were uni-seriate and support phialides on the upper two thirds of the vesicle. Conidia are globose to subglobose arose in chains, 4.5–6.5 μm in diameter, dark brown to black and roughened-walled (Table 4).

Fatty acids (FAs) profile analysis of AHM69 by GC/MS showed chain lengths of the fatty acid ranged from 8 to 22 carbons. The fungal lipids of AHM69 contain palmitic (C16:0), linoleic (C18:2), oleic (C18:1), linolenic (C18:3) and stearic (C18:0) acids as the dominant fatty acids that yielded 31.38 ± 0.78, 24.70 ± 4.30, 19.67 ± 0.34, 11.94 ± 0.16 and 10.41 ± 1.09% of the all fatty acids, respectively (Table 4). Other fatty acids such as caprylic (C8:0), lauric (C12:0), myristic (C14:0), palmitoleic (C16:1), margaric (C17:0), arachidic (C20:0) and behenic (C22:0) acids were also existing, but in amounts lesser than 1% as displayed in Table 4. Our data are in agreement with characterization of *Aspergillus* species

Table 6. Effect of different initial heavy metal concentrations on removal process efficiency by live biomass of *Penicillium* sp. AHM96 at various contact times.

Time (min)	*Concentration of heavy metal (mg/L)*											
	50		100		200		300		400		500	
	Removal (%)											
	Fe^{3+}	Co^{2+}	Fe^{3+}	Co^{2}+	Fe^{3+}	Co^{2+}	Fe^{3+}	Co^{2+}	Fe^{3+}	Co^{2+}	Fe^{3+}	Co^{2+}
10	57.51	100.0	66.00	90.35	40.99	77.80	25.16	70.40	19.22	68.06	10.61	51.30
30	84.50	100.0	76.93	100.0	60.25	100.0	39.53	89.56	27.81	75.81	19.42	59.11
60	100.0	100.0	90.22	100.0	71.19	100.0	58.99	100.0	41.20	84.35	30.00	62.43
120	100.0	100.0	96.50	100.0	77.80	100.0	70.25	100.0	53.10	100.0	49.15	80.34
180	100.0	100.0	100.0	100.0	90.38	100.0	86.80	100.0	79.42	100.0	69.50	100.0
240	100.0	100.0	100.0	100.0	85.42	100.0	81.38	100.0	74.93	100.0	62.20	100.0
300	100.0	100.0	93.16	100.0	85.42	100.0	81.19	100.0	71.19	100.0	61.50	100.0
360	100.0	100.0	90.56	100.0	80.81	100.0	80.42	100.0	64.70	100.0	60.21	100.0
420	100.0	100.0	90.20	100.0	80.80	100.0	74.56	100.0	60.16	100.0	49.16	100.0
1440	80.95	100.0	70.51	100.0	62.15	100.0	50.04	100.0	34.60	100.0	27.00	100.0

based on fatty acid profiles done by Fraga et al. (2008). Furthermore, the isolate AHM96 was recognized as *Penicillium* strain based on its phenotypic and cellular fatty acid analysis as described previously (Tiwari et al., 2011).

On Czapek's agar, AHM96 colonies were circular, concave in centers, texture velvety; blue-green surface but reverse yellowish brown with buff centers (Table 4). Very dense sporulation but no soluble pigments and exudates were detected (Table 4). Conidiophores were hyaline, biverticillate; supporting phialides in brush-like clusters; stipes septate, smooth-walled and 100–135 × 4–6 μm in diameter. 5–8 Phialides from branched cylindrical metulae (10.5–15.0 × 3.5–4.5μm) were formed at the ends of the conidiophores. Phialides are flask-shaped, composed of a cylindrical basal part and a distinct neck with diameter 9.0–12.0 × 3.3–4.0 μm. Moreover, Conidia are dull green, ellipsoidal, smooth-walled in long dry chains (Table 4). The chain lengths of the fatty acid profile for AHM96 isolate ranged from 14 to 20 carbons but the most common and abundant FAs extracted were linoleic acid (C18:2), oleic acid (C18:1), stearic acid (C18:0), palmitic acid (C16:0) and pentadecanoic (C15:0) which comprised 39.63 ± 1.09, 20.10 ± 0.54, 16.33 ± 0.81, 11.87 ± 0.59 and 8.03 ± 0.50% of the total peak area for the *Penicillium* strain AHM96 under study, respectively. In addition, small amounts of myristic (C14:0), palmitoleic (C16:1), margaric (C17:0), margaroleic (C17:1, w8), arachidic (C20:0), eicosenoic (C20:1) and eicosadienoic acids (C20:2) in the fatty acid profile of the fungal strain AHM96 (Table 4).

Recently the cellular FAs profile analysis is assist as beneficial chemotaxonomic tool for the identification, classification and differentiation of numerous species of filamentous fungi as *Fusarium*, *Aspergillus*, *Penicillium*, *Trichoderma*, *Acremonium*, and *Alternaria* species (Zain et al., 2013; El-Gendy et al., 2017). In line with our data Dusengemungu et al. (2020) and Hassouna et al. (2018) stated that numerous filamentous fungal strains have been isolated, recognized and evaluated for their heavy metals biosorption capability for potential application in bioremediation of Fe^{3+} and Co^{2+} wastes to find suitable candidates for biosorption, among them *Penicillium* and *Aspergillus* species have higher Fe^{3+} and Co^{2+} biosorption capability compared to other fungal species isolated as *Geotrichum*, *Monilia* and *Fusarium*.

3.5. Phylogenetic analysis and molecular identification of promising isolates AHM69 and AHM96

Molecular identification of selected fungi AHM69 and AHM96 were achieved by ITS site of the nuclear rDNA sequencing technique. The analysis of the got sequences was compared with that in the NCBI Nucleotide Sequence Database by the BLAST algorithm. A BLAST analysis performed via blastn search through GenBank displayed that the fungal isolates AHM69 and AHM96 belonged to Ascomycota. Isolate AHM69 belonged to genus *Aspergillus* was clustered together with *Aspergillus* sp. 39 (99.42%) as well as *A. cristatus* DUCC5705, *A. amstelodami* DUCC5704, *A. chevalieri* DTO 401-E8 and *A. glaucus* UBOCC-A-118067 (99.05%) (Figure 1). On the other hand, isolate AHM96 belonged to genus *Penicillium* that was much similar to *P. chrysogenum* air 7 and *P. granulatum* 67 (99.28%) (Figure 1). The sleeted isolates were initially recognized based on their morphological and biochemical properties followed by phylogenetic analysis of their

Table 7. Effect of different biosorbent dosages (%) on heavy metals removal process efficiency (%) by live biomass of *Aspergillus* sp. AHM69 and *Penicillium* sp. AHM96 after 180 min contact time.

Biosorbent	Heavy metal	Heavy metal conc. (mg/L)	Biosorption efficiency (%) at various biosorbent dosages (%)						
			0.05	0.1	0.2	0.3	0.4	0.5	1.0
Aspergillus sp. AHM69	Fe^{3+}	400	20.00	30.83	51.32	82.20	100.0	100.0	100.0
		500	31.76	43.00	60.18	78.00	100.0	100.0	100.0
		1000	29.98	34.16	44.65	63.85	87.98	100.0	100.0
	Co^{2+}	400	10.21	19.62	30.48	59.70	86.19	86.19	86.19
		500	10.00	19.00	30.40	50.24	73.11	73.11	73.11
		1000	12.00	15.16	22.14	27.93	30.24	34.18	40.04
Penicillium sp. AHM96	Fe^{3+}	400	18.86	29.91	47.50	58.30	79.42	80.95	91.00
		500	17.90	23.16	40.90	50.90	69.50	74.22	80.50
		1000	12.43	20.28	22.16	30.00	35.26	39.13	45.96
	Co^{2+}	400	39.89	50.60	70.29	90.10	100.0	100.0	100.0
		500	30.66	38.95	56.50	80.54	100.0	100.0	100.0
		1000	17.90	29.16	48.16	75.28	90.16	100.0	100.0

Table 8. Removal efficiency (%) of different contaminants and metal ions from the real refining wastewater at different locations by live biomass of *Aspergillus* sp. AHM69 and *Penicillium* sp. AHM96 under optimized conditions.

Parameter	Bioremoval efficiency (RE%)					
	Mostorod refining wastewater (Cairo)		America refining wastewater (Alexandria)		Tanta refining wastewater (Delta)	
	AHM69	AHM96	AHM69	AHM96	AHM69	AHM96
Calcium (Ca^{2+})	100.00 ± 0.39	100.00 ± 0.32	100.00 ± 0.44	100.00 ± 0.32	100.00 ± 0.40	100.00 ± 0.50
Potassium (K^{+})	79.18 ± 0.74	90.45 ± 0.98	76.61 ± 0.90	85.90 ± 0.70	80.35 ± 0.74	92.52 ± 0.86
Magnesium (Mg^{2+})	61.15 ± 0.30	76.54 ± 0.69	64.19 ± 0.38	80.24 ± 0.60	59.06 ± 0.29	73.46 ± 0.70
Sodium (Na^{+})	95.60 ± 0.79	90.25 ± 0.82	92.22 ± 0.73	90.11 ± 0.81	98.23 ± 0.90	93.08 ± 0.94
Aluminum (Al^{3+})	100.00 ± 0.67	100.00 ± 0.60	100.00 ± 0.73	100.00 ± 0.68	100.00 ± 0.70	100.00 ± 0.69
Iron (Fe^{3+})	100.00 ± 0.32	68.25 ± 0.20	100.00 ± 0.38	74.12 ± 0.24	100.00 ± 0.47	60.15 ± 0.30
Manganese (Mn^{2+})	100.00 ± 1.11	100.00 ± 0.98	100.00 ± 1.21	100.00 ± 0.99	100.00 ± 1.16	100.00 ± 0.94
Cupper (Cu^{2+})	100.00 ± 0.70	100.00 ± 0.75	100.00 ± 0.84	100.00 ± 0.79	100.00 ± 0.89	100.00 ± 0.69
Boron (B+)	84.13 ± 0.45	59.32 ± 0.24	79.02 ± 0.40	50.00 ± 0.20	73.41 ± 0.37	43.90 ± 0.25
Zinc (Zn^{2+})	100.00 ± 0.18	100.00 ± 0.24	100.00 ± 0.16	100.00 ± 0.19	100.00 ± 0.12	100.00 ± 0. 21
Barium (Ba^{2+})	36.86 ± 0.29	80.93 ± 0.50	45.20 ± 0.27	86.15 ± 0.60	34.59 ± 0.20	78.45 ± 0.73
Lead (Pb^{2+})	100.00 ± 1.02	100.00 ± 1.07	100.00 ± 1.11	100.00 ± 1.00	100.00 ± 0.92	100.00 ± 1.00
Cobalt (Co^{2+})	70.50 ± 0.38	100.00 ± 0.55	63.16 ± 0.30	100.00 ± 0.59	72.90 ± 0.44	100.00 ± 0.70
Nickel (Ni^{2+})	100.00 ± 0.45	100.00 ± 0.51	100.00 ± 0.60	100.00±±0.40	100.00 ± 0.44	100.00 ± 0.66
Arsenic (As^{3+})	100.00 ± 0.70	100.00 ± 0.56	100.00 ± 0.77	100.00 ± 0.63	100.00 ± 0.84	100.00 ± 0.66
Cadmium (Cd^{2+})	86.20 ± 0.65	100.00 ± 0.84	80.19 ± 0.60	100.00 ± 0.90	84.59 ± 0.71	100.00 ± 0.95
Silver (Ag^{+})	60.90 ± 0.88	94.59 ± 0.71	52.18 ± 0.80	91.37 ± 0.84	60.00 ± 0.96	85.18 ± 0.90
Chromium (Cr^{6+})	100.00 ± 0.60	100.00 ± 0.84	100.00 ± 0.60	100.00 ± 0.84	100.00 ± 0.60	100.00 ± 0.84
Mercury (Hg^{2+})	90.18 ± 0.33	60.70 ± 0.28	86.40 ± 0.29	50.11 ± 0.20	88.30 ± 0.30	44.91 ± 0.35
TPHs	100.00 ± 0.90	100.00 ± 1.20	100.00 ± 1.01	100.00 ± 1.13	100.00 ± 1.08	100.00 ± 1.18
PAHs	100.00 ± 1.00	100.00 ± 0.90	100.00 ± 1.00	100.00 ± 0.96	100.00 ± 1.00	100.00 ± 1.06
Phenols	100.00 ± 0.17	100.00 ± 0.40	100.00 ± 0.35	100.00 ± 0.26	100.22 ± 0.32	100.00 ± 0.20
Benzene, toluene, xylene (BTX)	100.00 ± 0.17	100.00 ± 0.40	100.00 ± 0.35	100.00 ± 0.26	100.22 ± 0.32	100.00 ± 0.20

ITS1 and ITS4 region of rDNA. Consequently, based on these criteria, AHM69 and AHM96 fungal isolates could be recognized and designated as *Aspergillus* sp. AHM69 and *Penicillium* sp. AHM96 as well as forward sequences information were submitted to NCBI GenBank under accession number MZ496576 and MZ496589, respectively. Therefore, morphological and cultural properties as well as sequence analysis are considered to be necessary for the identification of fungi. The most prominent fungal phylogenetic markers are the ITS region of the nuclear rDNA, 28S and the 18S rRNA genes sequences (El-Gendy et al., 2018).

3.6. Optimization of the heavy metals removal process parameters by biomass of Aspergillus sp. AHM69 and Penicillium sp. AHM96

3.6.1. Effect of operation temperature on the bioremoval efficiency by live and dead biomasses

The analysis of fungal strains *Aspergillus* sp. AHM69 and *Penicillium* sp. AHM96 efficiency as biosorbents for removal of Fe^{3+} and Co^{2+} from aqueous solution at different temperatures in Figure 2 revealed that, the live biomass of both strains, individually was considered to be superior to dead ones for Fe^{3+} and Co^{2+} removal. Bioremoval capacity of Fe^{3+} and Co^{2+} from aqueous solution was increased by 38.90 and 77.08% with the active cells of *Aspergillus* sp. AHM69 and by 29.25 and 24.65%, respectively with live biomass of *Penicillium* sp. AHM96 as compared to their dead counterparts at 40 °C (Figure 2). In accordance with our findings, Vacar et al. (2021) reported that live biomasses of a great number of filamentous fungi native to heavy metals (HMs) polluted region including *Didymella glomerata*, *Phoma costaricensis*, *Stagonosporopsis* sp., *Cladosporium* sp., *Aspergillus* sp., *Penicillium* sp., *Mortierella* sp., *Cadophora malorum*, *Sarocladium* sp., *Fusarium* sp. and *Lecanicillium* sp. have great potential for bioremediation, yet are still often underexploited due to higher number of binding sites and functional groups that enhancing its stability, settling property and heavy metals uptake capacities of the biomass.

Moreover, the removal efficiency of Fe^{3+} and Co^{2+} by the live biomass of *Aspergillus* sp. AHM69 was increased by 25.27 and 19.81% when the process temperature increased from 40 °C to 45–55 °C (Figure 2). On the other hand, bio-adsorption of Fe^{3+} and Co^{2+} by the live biomass of *Penicillium* sp. AHM96 was increased from 51.7 and 79.15% at 40 °C to 53.94 and 90.34% at 45 °C (Figure 2). Removal efficiency by both fungal biomasses was decreased at higher or lower temperatures. Ayele et al. (2021) reported that the increase in temperature improves the biosorption rate of iron and reduces the contact time required for removal of heavy metals by fungi as it affects the cell wall configuration, stability and permeability of components resulting in better diffusion of metals within the pores and improves the mobility of metals from the aqueous solution. In addition, it creates new active sites on the sorbent to the adsorbent surface, increases the chemical affinity between the metal cations and the adsorbent surface and it is an important parameter for energy dependent mechanisms in the biosorption process.

3.6.2. Effect of different pH values on the bioremoval process by live and dead biomass

Removal of metal ions from aqueous solution strongly depends on the pH of the solution, it affects both the ionization state of functional groups (amino, carboxylic and phosphate groups) on fungal cell walls and the solubility of metal ions (Koul et al., 2021). In the current work by increasing pH from 3.0 to 4.5–5.0, bioremoval ability of the live biomass of *Aspergillus* sp. AHM69 toward Fe^{3+} and Co^{2+} were increased by 3.984- and 4.122-fold, respectively as well as increased by 5.473- and 3.507-fold with its dead biomass at pH 5.0, respectively (Figure 3). Moreover, the bioremoval efficiency of Fe^{3+} and Co^{2+} by *Penicillium* sp. AHM96 increased from 19.30 and 47.15% at pH 3.0 to 75.4 and 100% at pH 5.0, respectively with its live biomass but using its dead biomass increased the removal percentage of Fe^{3+} and Co^{2+} from 10.90 and 30.15% at pH 3.0 to 55.20 and 90.0%, respectively at pH 5.0 (Figure 3). Then using live biomass of AHM69 at pH 4.5–5.0 supported the highest removal of Fe^{3+} and Co^{2+} while live biomass of AHM96 required pH 5.0 to reach the highest adsorption capacity for two heavy metals from their aqueous

solutions (Figure 3). At higher or lower pH than the optimal range, the biosorption capacity of both strains by their two forms (live and dead biomasses) toward the two heavy metals was significantly decreased (Figure 3). These explanations agree with those stated in previous studies. Alyasi et al. (2020) displayed that heavy metal adsorption from aqueous solution increases with increasing pH up to pH 5.0 and then decreased due to the positive surface charge at pH values <5 results in H^+ ions competing with heavy metal for sorption sites, which leads to a decrease in adsorption but at higher pH values ˃ 5, metals begin to precipitate due to the formation of metal hydroxides complexes that decrease the efficiency of the metal removal. Accordingly, the dried live biomasses of *Aspergillus* sp. AHM69 and *Penicillium* sp. AHM96 were selected for the further bioremoval studies.

3.6.3. Effect of initial concentrations of heavy metal versus variable contact times on the bioremoval capacity by live biomass

The initial concentration of heavy metal ions in the solution plays a major role as a driving force to overcome the mass transfer resistance between the aqueous and solid phases. The live biomass of *Aspergillus* sp. AHM69 reached equilibrium stage with an iron dose of 50, 100, (200 and 300), 400 and 500 mg/L within 10, 30, 60, 120 and 180 min, respectively (Table 5). Cobalt biosorption to reach equilibrium at concentrations of 50, 100 and 200 mg/L, it took 120, 180 and 300 min, respectively while at higher Co^{2+} concentrations such as 300, 400 and 500 mg/L, bioremediation process requires more than 24 h as contact times to reach the equilibrium point (Table 5). Hassouna et al. (2018) reported that bioabsorption of Fe^{3+} by *A. versicolor* was achieved at concentration of 90 ppm Fe^{3+} and then removal decreased with increase of Fe^{3+} concentration because higher concentrations make the sites available for sorption become fewer in comparison with the molecules of solute present. Interestingly adsorption process of Co^{2+} at 200 mg/L by AHM69 biomass was slow down with increasing the contact time, from 100% after 300 min to 63.14% after increasing contact time to 1440 min. Cobalt adsorption at 300, 400 and 500 mg/L by AHM69 biomass was decreased from 91.15, 86.19 and 73.11% to 50.21, 30.0 and 23.14%, respectively after increasing the operation time from 180 to 1440 min (Table 5). In line with our results Cárdenas González et al. (2019) mentioned that the percentage of adsorption decreased whenever Co^{2+} concentration increased from 300 to 600 mg/L through the biosorption of Co^{2+} by *Penicillium* sp. and *A. niger*.

Otherwise, the time profile of the heavy metals biosorption by the live biomass of *Penicillium* sp. AHM96 at various metal concentrations was smooth and continuous leading to saturation as shown in Table 6. Strain AHM96 achieved complete removal of iron (RE = 100%) at a concentration of 50 and 100 mg/L and reached the equilibrium stage after 60 and 180 min of treatment but it was able to remove 50, 100–200, 300, 400 and 500 mg/L of Co^{2+} in 10, 30, 60, 120 and 180 min, respectively (Table 6). The adsorption efficiency of iron at 50, 100, 200, 300, 400 and 500 mg/L by AHM96 was decreased from (100%–80.95%), (100%–70.51%), (90.38%–62.15%), (86.80%–50.04%), (79.42%–34.60%), and (69.50%–27.0%) after increasing the contact time from 180 to 1440 min, respectively (Table 6). The decreasing of adsorption capability of heavy metals into fungal biomass by increasing the contact time was previously reported by Kanamarlapudi et al. (2018) they stated that the rate of biosorption metal ion is rapid in the initial period with approximately 90% of the active metal-binding sites being free and accessible for biosorption but with the increasing time, the biosorption efficiency decreases because of the higher saturation of metal ions remaining in the solution.

3.6.4. Effect of the fungal biosorbent dosage

As shown in Table 7, the removal rapidly increased for Fe3+ from 20.0% to 100% and Co^{2+} from 10.21% to 86.19% at 400 mg/L of each metal concentration, individually after increasing the biomass dose of *Aspergillus* sp. AHM69 from 0.05% to 0.4% in the removal process. At a higher concentration equal to 1000 mg/L of Fe^{3+} and Co^{2+}, we observed an increase in the removal efficiency of Fe^{3+} from 29.98% to 100.0% and Co^{2+} from 12.0% to 40.04% after increasing the dose of AHM69 biosorbent from 0.05% to 0.5% and 1.0%, respectively (Table 7). Hassouna et al. (2018) indicated that the increase in the biomass dosage of *A. versicolor* biosorbent concentrations from 0.05 to 0.5 g resulted in excessive increase in the Fe^{3+} removal efficiency and reaching equilibrium quickly due to the increase of the adsorption surface area and availability of free adsorption sites that help in iron removal. Regarding the live biomass of *Penicillium* sp. AHM96, Fe^{3+} removal at a concentrations of 400, 500 and 1000 mg/L was increased from 18.86, 17.90 and 12.43% to 91.00, 80.50 and 45.96%, respectively, after increasing the concentration of the adsorbent *Penicillium* sp. AHM96 from o.05%–1.0% while the removal efficiency of Co^{2+} at the same concentrations of 400, 500 and 1000 mg/L was increased from 39.89, 30.66 and 17.90% at a biomass dose of 0.05%–100% removal with a biomass amount equal to 0.5% (Table 7). The increase in the heavy metals removal capacity is mainly attributed to the amount of the added fungal biosorbents fixed, which increases the available number of binding sites and the adsorption surface area of the fungal biomass of *Trichoderma viride*, *A. flavus*, *A. niger*, *A. tamari*, *P. brevicompactum*, *P. citrinum* and *Penicillium* sp. 104 for the adsorption of metals (Dusengemungu et al., 2020; Ayele et al., 2021).

3.7. Removal of different contaminants and metal ions from petroleum refining effluents by the live biomass of Aspergillus sp. AHM69 and Penicillium sp. AHM96 under optimized conditions

Data in Table 8 indicated that the optimization of removal process parameters efficiently increased the removal capacity of both strains toward the metal ions and other contaminants present in the wastewater of Mostorod, America and Tanta refineries. Both *Aspergillus* sp. AHM69 and *Penicillium* sp. AHM96 strains were able to entirely remove (100%) of Ca^{2+}, Al^{3+}, Mn^{2+}, Cu^{2+}, Zn^{2+}, Pb^{2+}, Ni^{2+}, As^{3+}, Cr^{6+}, TPHs, PAHs, BTX and phenols (Table 8). Total removal of Co^{2+} and Cd^{2+} was achieved by the live biomass of *Penicillium* sp. AHM96 but the total adsorption of Fe^{3+} from petroleum effluents was recorded with the active cells of *Aspergillus* sp. AHM69. Furthermore, the biomass of *Aspergillus* sp. AHM69 showed higher affinity toward the metal ions Na^+ (RE = 92.22 ± 0.73–98.23 ± 0.90%), B^+ (RE = 73.41 ± 0.37–84.13 ± 0.45%), and Hg^{2+} (RE = 86.40 ± 0.29–90.18 ± 0.33%) while the *Penicillium* sp. AHM96 was the most active biosorbent for K^+ (RE = 85.90 ± 0.70–92.52 ± 0.86%) Ba^{2+} (RE = 78.45 ± 0.73–86.15 ± 0.60%) and Ag^+ (RE = 85.18 ± 0.90–94.59 ± 0.71%) (Table 8). Herein the present study represents two potent biological remediation agents *Aspergillus* sp. AHM69 and *Penicillium* sp. AHM96 as low cost biosorbents for different heavy metals and hydrocarbons from wastewater. Similar results were reported on the removal and uptake of heavy metals from real industrial wastewater under optimized conditions by *Actinomycetes* such as *Nocardia* and *Nocardiopsis* species (El-Gendy and El-Bondkly, 2016) as well as by a large number of fungi including *D. hawaiiensis*, *Fusarium* sp. #ZZF51, *Penicillium lilainum*, *Alternaria alternate*, *Mucor rouxi*, *Trametes versicolor*, *Aspergillus fumigatus*, *Rhizopus arrhizus*, *Lentinus edodes*, *Aspergillus niger*, *Pleurotus ostreatus*, *Cladosporium resinae* and *Paecilomyces variotii* (El-Gendy et al., 2011, 2017; Alzahrani and El-Gendy, 2019; Ayele et al., 2021).

3.8. Fourier-transform infrared spectroscopy analysis (FTIR absorptions) for functional groups of fungal biomasses

FTIR analysis indicated the variations induced by heavy metals under study in functional groups on biomass surface. The biosorption mechanism is essentially based on physicochemical interactions between metal ions and functional groups. Characteristic infrared peaks of metal-loaded and unloaded *Aspergillus* sp. AHM69 as well as *Penicillium* sp. AHM96 biomasses acquired inside the range of 450–4000 cm^{-1} displayed some shifts and changes in the adsorption peaks, indicating the interactions between each functional group of each strain and heavy metals under study have been occurred (Figure 4). Unloaded AHM69 biomass

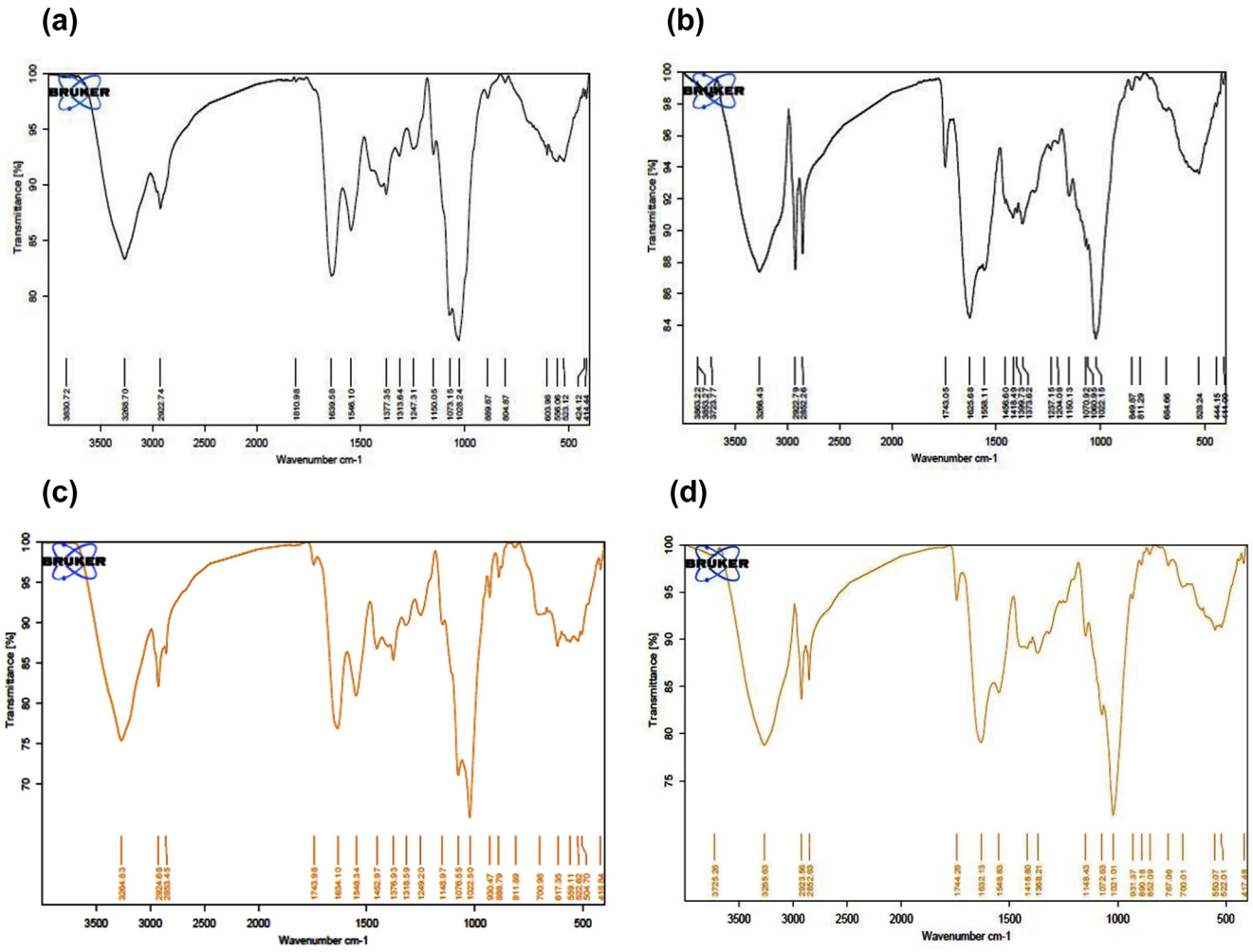

Figure 4. FTIR absorptions analysis for functional groups of unloaded (a and c) and loaded (b and d) *Aspergillus* sp. AHM69 and *Penicillium* sp. AHM96 biomasses, respectively.

exhibited a characteristic broad peak at 3268.70 cm^{-1} (3600-3100 cm^{-1}) indicative of a strong O–H stretch, hydrogen bonded and a strong stretching vibration of the N–H amine. Additional peaks at 2922.74 cm^{-1} could be medium C–H symmetric stretching, 1810.98 cm^{-1} refer to strong C=O stretching (anhydride), sharp bands at 1639.58 cm^{-1} (1650-1600 cm^{-1}) and 1546.10 cm^{-1} (1560-1500 cm^{-1}) could be denote medium C=C stretching (a conjugated alkene) and a strong N–O stretching (nitro compound), respectively (Figure 4). Moreover, bands detected at 1377.35 and 1313.64 cm^{-1} indicating medium O–H bending (phenol) along with the other bands detected at 1247.31, 1150.05, 1073.15 and a long sharp band at 1028.24 cm^{-1} that might be indicative of the medium C–N stretching amine. Additional peaks in the unloaded AHM69 biomass at 889.87, 804.87, (603.98, 556.06 and 523.12 cm^{-1}), and (424.12 and 414.44 cm^{-1}) could be strong C=C bending (alkene), medium C=C bending (alkene), strong C–Br stretching and strong C–I stretching (halo compound) (Figure 4a). On the other hand, the biomass of AHM69 loaded with Fe^{3+} and Co^{2+} showed several new peaks positions at 3863.22, 3853.27 and 3723.77 cm^{-1} (strong water OH stretch); 2852.26 cm^{-1} (C–H stretch, alkanes); 1456.60, 1418.49, 1399.73 and 1373.62 cm^{-1} (medium CH_3 bend); 1204.08 cm^{-1} (strong C–O stretching tertiary alcohol) and 1060.95 cm^{-1} (strong S=O stretching sulfoxide) (Figure 4b). Furthermore, the peaks at 849.87 and 811.29 cm^{-1} indicate a strong C–Cl stretching; 684.66 and 528.24 cm^{-1} could be strong C–Br stretching along with 444.15 and 411.09 cm^{-1} indicating strong C–I stretching were detected and refer to forming halo compound while peaks at 603.98, 556.06 and 424 cm^{-1} were not detected in the AHM69 biomass after adsorption (Figure 4b). However, in the loaded AHM69 biomass with the heavy metals the peaks at 3268.70, 2922.79 and 1810.98 cm^{-1} (C=O stretching anhydride) shifted to 3266.43 cm^{-1}, sharp peak at 2922.79 cm^{-1} and 1743.05 cm^{-1} that may refer to strong C=O stretching ketone while peaks at 1639.58 cm^{-1} (1650-1600 cm^{-1}) and 1546.10 cm^{-1} were shifted to 1625.68 cm^{-1} (1650-1580 cm^{-1}, referring to medium N–H bending amine) and 1558.11 cm^{-1}, respectively (Figure 4b). In addition, the peak at positions 1247.31, 1150.05, 1073.15 and 1028.24 cm^{-1} shifted to 1237.15, 1150.13, 1070.92 and 1022.15 cm^{-1}, respectively (medium C–N stretching amine) (Figure 4b).

Interestingly, the characteristic IR absorption peaks of the functional groups in the unloaded biomass compared to the loaded biomass of AHM 96 strain showed that the characteristic bands at 1452.97 cm^{-1} (medium C–H bend alkanes), 1376.93 cm^{-1} (medium CH3 bend), 1318.59 cm^{-1} (strong C–N stretching aromatic amine), 1249.20 cm^{-1} (medium C–N stretching amine), 811.89 cm^{-1} (medium C=C bending alkene), 617.35 cm^{-1} (strong C–Br stretching halo compound) and 504.70 cm^{-1} (strong C–I stretching) in the unloaded biomass were not detected in the loaded biomass AHM 96 with Fe^{3+} and Co^{2+} (Figure 4c, d). Conversely, new characteristic peaks include 3725.26 cm^{-1} (strong water OH Stretch), 1418.80 cm^{-1} (medium O–H bending alcohol), 1368.21 cm^{-1} (strong S=O stretching sulfonamide), 852.09 and 767.06 cm^{-1} (strong C–Cl stretching, halo compound) were recorded in AHM 96 loaded biomass (Figure 4c, d). Moreover the peaks at 3264.83, 2924.68, 2853.45, 1743.98, 1634.10, 1548.34, 1148.97, 1076.55, 1022.50, 930.47, 888.79, 700.98, 559.11, 522.62 and 418.84 cm^{-1} were slightly shifted to

3265.63 cm^{-1} (strong O–H stretching carboxylic acid), 2923.56 and 2852.63 cm^{-1} (medium C–H stretching alkane), 1744.26 cm^{-1} (strong C=O stretching cyclopentanone), 1632.13 cm^{-1} (medium C=C stretching alkene), 1548.83 cm^{-1} (strong N–O stretching nitro compound), 1148.43 cm^{-1} (medium C–N stretching amine), 1072.63 cm^{-1} (strong C–O stretching primary alcohol), 1021.01 cm^{-1} (medium C–N stretching amine), 931.37 cm^{-1} (strong C=C bending alkene), 890.18 cm^{-1} (strong C=C bending alkene), 700.01 cm^{-1} (strong C–Cl stretching halo compound), 550.07 and 522.01 cm^{-1} (C–Br stretching) and 417.48 cm^{-1} (strong C–I stretching), respectively (Figure 4c, d). Zhang et al. (2020) reported that the changes in the vibrational frequencies studied by FTIR analysis on the surface of metal-treated fungus supported the involvement of biosorption for metal removal, the biosorption mechanisms are mainly based on physicochemical interactions between the metal ions and the functional groups and the type of functional groups present depended on the fungal species. For example, Cu, Cr, Cd, Pb, Zn and Fe removal by *Trichoderma brevicompactum* QYCD-6 involved saccharides hydroxyl, carboxylate and disulphide groups of nitro compounds; lead removal by *Beauveria bassiana* involved protein, carbohydrate, fatty acids esters and protein amide groups while the uptake of silver by *Fusarium solani* was attributed to hydroxyl, amines/amides, carboxylic acid and phosphatidate functional groups (El-Sayed and El-Sayed, 2020).

3.9. Scanning electron microscopy and energy dispersive X-ray spectrometry (SEM-EDX) analysis of Aspergillus sp. AHM69 and Penicillium sp. AHM96 biomasses before and after treatment with Fe^{3+} and Co^{2+} heavy metals

Assessment of morphological changes in response to iron and cobalt accumulated in the biomass of fungal strains, *Aspergillus* sp. AHM69 and *Penicillium* sp. AHM96 as well as iron and cobalt quantification within fungal biomasses were performed by scanning electron microscopy (SEM) and energy dispersive X-ray analysis (EDX) (Figure 5). By comparing the SEM images of the unloaded cells of *Aspergillus* sp. AHM69 strain, which are characterized by the regular and homogeneous shape of the cells in Figure 5a with that treated with a mixture of cobalt and iron heavy metals in Figure 5b we observed a detectable alteration in morphology between the fungi grown in the control condition and in the

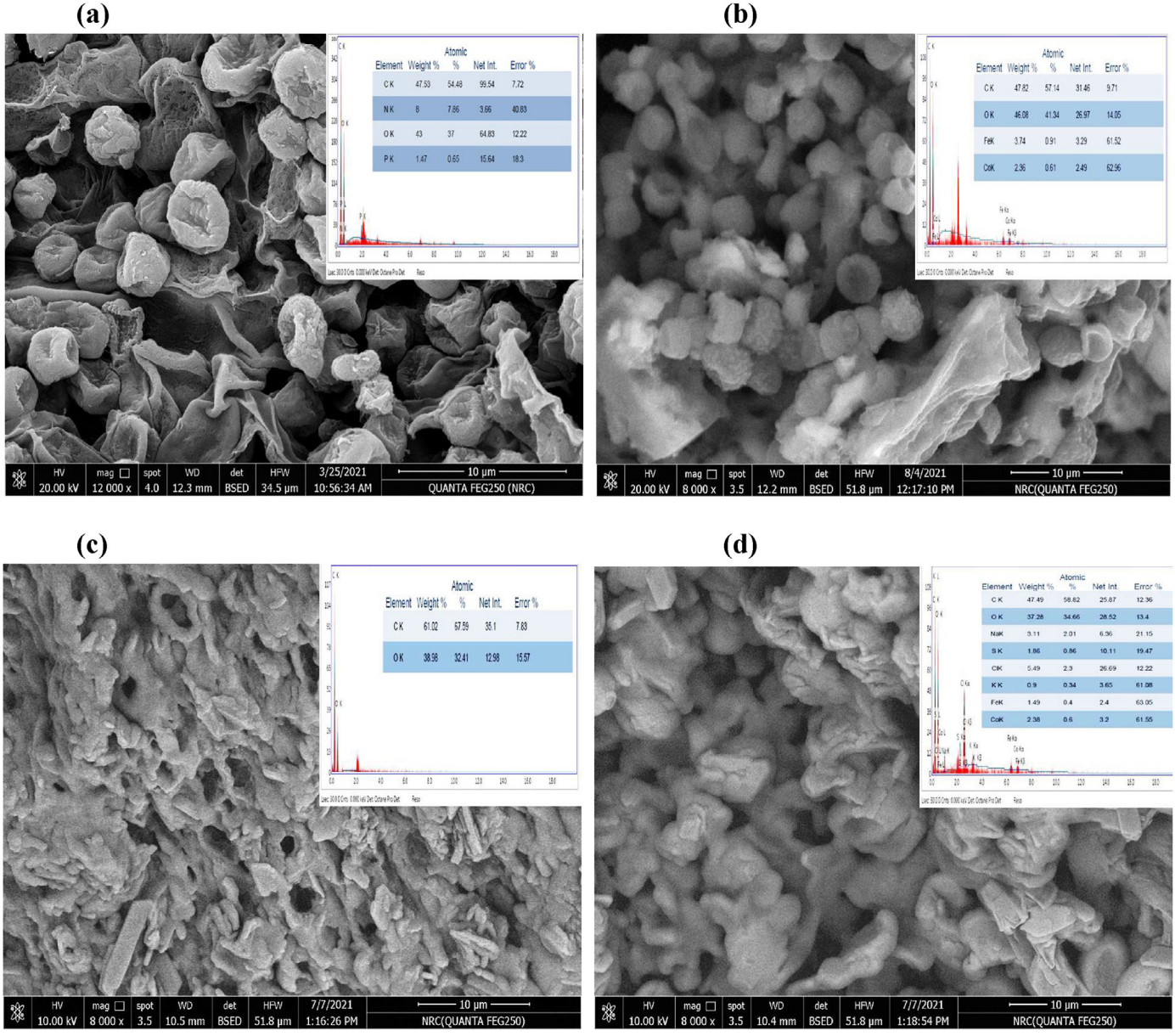

Figure 5. SEM-EDX of *Aspergillus* sp. AHM69 and *Penicillium* sp. AHM96 (a and c) control (b and d) in the presence of iron and cobalt, respectively.

presence of Fe^{3+} and Co^{2+} such as clear deformation, indentations in cells especially in the middle, more dense, packed tightly and clear and regular aggregations in addition to shrinking cells with shrunken cell walls after treatment with Fe^{3+} and Co^{2+} (Figure 5a and b).

On the other hand, the morphology of *Penicillium* sp. AHM96 in the absence of Fe^{3+} and Co^{2+} showed a regular and uniform fungal shape (Figure 5c) but after treatment with Fe^{3+} and Co^{2+} we noticed that severe deformation, flattening, some distortions, elongation, enlargement of the size of the cells and their agglomeration in the form of irregular masses were occurred in the presence of Fe^{3+} and Co^{2+} (Figure 5d). Interestingly *Penicillium* sp. AHM96 showed much higher morphological abnormalities than *Aspergillus* sp. AHM69 strain after treatment with both cobalt and iron. Moreover, some shinny small particles that were observed over the surface of Fe^{3+}- and Co^{2+}-loaded biomass of AHM69 and AHM96 strains but they were absent on the surface of the unloaded biomasses (Figure 5a, b, c, d). These morphological abnormalities changes in each fungal biomass caused by Co^{2+} and Fe^{3+} absorption indicate the toxic effects of these heavy metals on the fungal strains under study. They might be the toxicity response of *Aspergillus* sp. AHM69 and *Penicillium* sp. AHM96 against Fe^{3+} and Co^{2+}. These findings are in line with many previous reports such as Gururajan and Belur (2018) and Chen et al. (2014), they stated that Heavy metal uptake and accumulation cause many damages at morphological, cellular, physiological and molecular levels containing ultra-structural changes, protein and DNA oxidation as well as inhibition of antioxidative systems in living cells. Moreover, hyphal aggregation in the presence of heavy metals might be a strategy to overcome these toxic effects of heavy metals by reducing the total surface area of the fungi exposed to heavy metals.

Parallel morphological alterations in the presence of heavy metals were detected with other fungal species such as *Aspergillus foetidus*, *A. niger* and *Beauveria bassiana* using SEM-EDX as rapid, cost effective and successful procedure to study and explain tolerance of fungi to heavy metals (Gola et al., 2018). These morphological alternations were explained by the EDX analysis data, which indicated heavy metals removal by AHM69 and AHM96 strains was via biosorption and bioaccumulation of a large amount of Fe^{3+} and Co^{2+} on cell surface (Figure 5a, b and c, d). EDX spectra of unloaded fungal biomass of *Aspergillus* sp. AHM69 (Figure 5a) and *Penicillium* sp. AHM96 (Figure 5c) showed no peaks for iron and cobalt before exposure of biomass to these heavy metals but detectable peaks of Fe^{3+} and Co^{2+} were observed after they were exposure to these heavy metals (Figure 5b, d), which indicates the extracellular binding of these heavy metals on the cell surface of both strains rather than their intracellular accumulation on one hand and proposed the bioremoval of metals from aqueous solutions or petroleum refining effluents by biosorption and extracellular bioaccumulation as mechanisms in both fungal strains *Aspergillus* sp. AHM69 and *Penicillium* sp. AHM96. In line with our data, Chen et al. (2017) reported that SEM-EDX analysis proposed biosorption and bioaccumulation as mechanisms for Al (III), Cr (III) and Pb (II) removal by the fungal isolates *Simplicillium chinense*, *Penicillium simplicissimum*, *Trichoderma asperellum* and *Coriolopsis* sp.

4. Conclusions

Biological treatment of petroleum refining wastewater is an economical and effective method of waste stabilization. The fungal strains in the current work can be used as effective biological adsorbents for heavy metals, hydrocarbons and other toxic petroleum pollutants from wastewater generated by various petroleum industries, especially oil refining areas where bioremediation must be carried out by the indigenous organisms of oil-polluted environment that have developed methods to adapt to growth in their oily environment for decades. Isolation and application of certain fungi derived from the mycobiome in the contaminated area to treat recalcitrant compounds can be a topic in the future for effective removal of non-degradable wastes such as heavy metals and cyclic aromatic hydrocarbons in the petroleum refining effluents. In the present work, twenty indigenous fungal isolates obtained from the mycobiome of different petroleum refining areas in Egypt including Mostorod north of the capital Cairo, Ameria in west Alexandria and Tanta in the Delta region were able to remove efficiently various pollutants from the aqueous solutions and real refinery effluents. Among them *Aspergillus* sp. AHM69 and *Penicillium* sp. AHM96 exhibited the hyper bioremediation activity against metal ions containing Na^{+}, K^{+}, Mg^{2+}, Ca^{2+}, Al^{3+}, Fe^{3+}, Mn^{2+}, Cu^{2+}, Zn^{2+}, Pb^{2+}, Co^{2+}, Ni^{2+}, As^{3+}, Cd^{2+} and Cr^{6+}. They also showed potent adsorption activity against BOD, TOC, COD, TSS, TDS, BTX, PAHs, TPHs, phenols, oil and grease along with decreasing, coloration and turbidity in the refineries effluents. Then *Aspergillus* sp. AHM69 and *Penicillium* sp. AHM96 can be employed as bioremediation agents to remove and/or degrade oil pollutants to restore the ecosystem when contaminated with oil. The removal process factors containing temperature, pH, initial metal concentration, contact time, the biomass dose and form of biomass (live or dead biomass) were optimized to achieve the best removal of iron and cobalt, which were recorded as the top pollutants in the refineries effluents under study.

Declarations

Author contribution statement

Ahmed Mohamed Ahmed El-Bondkly & Mervat Morsy Abbas Ahmed El-Gendy: Conceived and designed the experiments; Performed the experiments; Analyzed and interpreted the data; Wrote the paper.

Funding statement

The research work was supported and funded by National Research Centre, Egypt [Project Number: 12030204]

Data availability statement

Data included in article/supp. material/referenced in article.

Declaration of interests statement

The authors declare no conflict of interest.

Additional information

No additional information is available for this paper.

Acknowledgements

Deep thanks and gratitude from the research team to the National Research Centre, Dokki, Giza, Egypt for fund, support and assistance this research work.

References

Aishwarya, S., Nagam, N., Vasudeva, N.R., Vijaya, T., 2017. Screening and identification of heavy metal-tolerant endophytic fungi *lasiodiplodia theobromae* from *boswellia ovalifoliolata* an endemic plant of Tirumala hills. Asian J. Pharm. Clin. Res. 10 (3), 488–491.

Al-Hawash, A.B., Zhang, X., Ma, F., 2019. Removal and biodegradation of different petroleum hydrocarbons Using the filamentous fungus *Aspergillus* sp. RFC-1. Microbiologyopen 8 (1), e00619.

Alyasi, H., Mackey, H.R., McKay, G., 2020. Removal of cadmium from waters by adsorption using nanochitosan. Energy Environ. 31 (3), 517–534.

Alzahrani, N.H., Alamoudi, K.H., El-Gendy, M.M.A.A., 2017. Molecular identification and nickel biosorption with the dead biomass of some metal tolerant fungi. J. Microb. Biochem. Technol. 9, 310–315.

Alzahrani, N.H., El-Gendy, M.M.A.A., 2019. Tolerance and removal of zinc (II) and mercury (II) by dead biomass of *Aspergillus tubingensis* merv4. Industrial Pollution Control 35 (1), 2251–2257.

American Public Health Association (APHA), 1995. Standard Method for the Examination of Water and Wastewater, nineteenth ed. Washington, DC, USA.

American Public Health Association (APHA), 1998. 2540 solids. In: Standard Methods for the Examination of Water and Wastewater, twentieth ed., pp. 2-54–2-60 Washington DC, USA.
American Public Health Association (APHA)/(AWWA), 2012. Standard Methods for the Examination of Water, and Wastewater, twenty-second ed. WPCF Washington DC, USA, p. 1360.
American Public Health Association (APHA), 2018. Standard Methods for the Examination of Water and Wastewater (SMWW), 23rd ed. Washington, DC, USA.
Ayele, A., Haile, S., Alemu, D., Kamaraj, M., 2021. Comparative utilization of dead and live fungal biomass for the removal of heavy metal: a concise review. Sci. World J. 2021, Article ID 5588111.
Ayers, R.S., Westcot, D.W., 1994. Food, Agriculture Organization of the United Nations (FAO). Water Quality for Agriculture, Irrigation and Drainage, Rome. Paper No. 29. Rev 1, M-56.
Biswal, N., Agrawal, A., 2016. Bioaccumulation of toxic metals through aquatic fungi. World J. Pharm. Pharmaceut. Sci. 5 (6), 1892–1901.
Brandão, P.C., Souza, T.C., Ferreira, C.A., Hori, C.E., Romanielo, L.L., 2010. Removal of petroleum hydrocarbons from aqueous solution using sugarcane bagasse as adsorbent. J. Hazard Mater. 175 (1-3), 1106–1112.
Burakov, A.E., Galunin, E.V., Burakova, I.V., Kucherova, A.E., Agarwal, S., Tkachev, A.G., Gupta, V.K., 2018. Adsorption of heavy metals on conventional and nanostructured materials for wastewater treatment purposes. A review, Ecotoxicology and Environmental Safety 148, 702–712.
Canadian Council of Ministers of the Environment (CCME), 1999. Canadian Environmental Quality Guidelines, Winnipeg, 2007, 2011.
Canadian Council of Ministers of the Environment (CCME), 2014. Canadian Water Quality Guidelines: Cadmium. Scientific Criteria Document, Winnipeg.
Cárdenas González, J.F., Rodríguez Pérez, A.S., Vargas Morales, J.M., Martínez Juárez, V.M., Rodríguez, I.A., et al., 2019. Bioremoval of cobalt (II) from aqueous solution by three different and resistant fungal biomasses. Bioinorgan. Chem. Appl. 8, 2019, Article ID 8757149.
Chen, A., Zeng, G., Chen, G., Liu, L., Shang, C., Hu, X., Lu, L., Chen, M., et al., 2014. Plasma membrane behavior, oxidative damage, and defense mechanism in *Phanerochaete chrysosporium* under cadmium stress. Process Biochem 49, 589–598.
Chen, S.H., Ng, S.L., Cheow, Y.L., Ting, A.S.Y., 2017. A novel study based on adaptive metal tolerance behavior in fungi and SEM-EDX analysis. J. Hazard Mater. 334, 132–141.
Decree of Health Ministry, 2007. Egyptian Standards for Drinking Water and Domestic Uses, (No. 458).
Dincer, A.R., Karakaya, N., Gunes, E., Gunes, Y., 2008. Removal of COD from oil recovery industry wastewater by the advanced oxidation processes (AOP) based on H_2O_2. Glob. N. J. 10, 31–33.
Dusengemungu, L., Kasali, G., Gwanama, C., Ouma, K.O., 2020. Recent advances in biosorption of copper and cobalt by filamentous fungi. Front. Microbiol. 11, 582016.
El-Bondkly, A.M.A., 2012. Molecular identification using ITS sequences and genome shuffling to improve 2- deoxyglucose tolerance and xylanase activity of marine-derived fungus, *Aspergillus sp.* NRCF5. Appl. Biochem. Biotechnol. 167 (8), 2160–2173.
El-Gendy, M.M.A.A., El-Bondkly, A.M.A., 2016. Evaluation and enhancement of heavy metals bioremediation in aqueous solutions by *Nocardiopsis sp.* MORSY1948, and *Nocardia sp.* MORSY2014. Braz. J. Microbiol. 47 (3), 571–586.
El-Gendy, M.M.A., Hassanein, N.M., Ibrahim, H.A., Abd El-Baky, D.H., 2011. Evaluation of some fungal endophytes of plant potentiality as low-cost adsorbents for heavy metals uptake from aqueous solution. Australian Journal of Basic and Applied Sciences 5 (7), 466–473.
El-Gendy, M.M.A.A., Hassanein, N.M., Ibrahim, H.A., Abd El-Baky, D.H., 2017. Heavy metals biosorption from aqueous solution by endophytic *Drechslera hawaiiensis* of *Morus alba* L. derived from heavy metals habitats. MYCOBIOLOGY 45 (2), 73–83.
El-Gendy, M.M.A.A., Yahya, S.M.M., Hamed, A.R., Soltan, M.M., El-Bondkly, A.M.A., 2018. Phylogenetic analysis and biological evaluation of marine endophytic fungi derived from Red Sea sponge *Hyrtios erectus*. Applied biochemistry and biotechnology 185 (3), 755–777.
El Sayed, M.T., El-Sayed, A.S.A., 2020. Tolerance and mycoremediation of silver ions by Fusarium solani. Heliyon 6 (2020), e03866.
Engwa, G.A., Ferdinand, P.U., Nwalo, F.N., Unachukwu, M.N., 2019. Mechanism and Health Effects of Heavy Metal Toxicity in Humans, Poisoning in the Modern World - New Tricks for an Old Dog?, Ozgur Karcioglu and Banu Arslan. IntechOpen.
Fraga, M.E., Santana, D.M., Gatti, M.J., et al., 2008. Characterization of *Aspergillus* species based on fatty acid profiles. Mem. Inst. Oswaldo Cruz 103 (6), 540–544.
Gola, D., Malik, A., Namburath, M., et al., 2018. Removal of industrial dyes and heavy metals by *Beauveria bassiana*: FTIR, SEM, TEM and AFM investigations with Pb(II). Environ. Sci. Pollut. Res. 25, 20486–20496.
Gururajan, K., Belur, P., 2018. Screening and selection of indigenous metal tolerant fungal isolates for heavy metal removal. Environ. Technol. Innov. 9 (2018), 91–99.
Hassouna, M.E.M., Marzouk, M.A., Elbably, M.A., et al., 2018. Biosorption of iron by amended *Aspergillus versicolor* from polluted water sources. Biom. Biostat. Int. J. 7 (6), 502–513.
Ishak, S., Malakahmad, A., 2013. Optimization of fenton process for refinery wastewater biodegradability augmentation. Korean J. Chem. Eng. 30 (5), 1083–1090.
Kanamarlapudi, S.L.R.K., Chintalpudi, V.K., Muddada, S., 2018. Application of biosorption for removal of heavy metals from wastewater. Biosorption 18, 69.
Kidd, S., Halliday, C., Alexiou, H., Ellis, D., 2016. Descriptions of Medical Fungi. Newstyle Printing, South Australia.
Koul, B., Ahmad, W., Singh, J., 2021. Microbe Mediated Remediation of Environmental Contaminants. Chapter 30 – Mycoremediation: A Novel Approach for Sustainable Development. Woodhead Publishing Series in Food Science, Technology and Nutrition, pp. 409–420.
Kumar, A., Kumar, V., Singh, J., 2019. Role of fungi in the removal of heavy metals and dyes from wastewater by biosorption processes. In: Yadav, A., Singh, S., Mishra, S., Gupta, A. (Eds.), Recent Advancement in White Biotechnology through Fungi. Fungal Biology. Springer.
Kumar, S., Stecher, G., Li, M., Knyaz, C., Tamura, K., 2018. Mega X: molecular evolutionary genetics analysis across computing platforms. Mol. Biol. Evol. 35, 1547–1549.
Larone, D.H., 1995. Medically Important Fungi. A Guide to Identification, third ed. American Society for Microbiology Press, Washington, D.C. USA.
Liu, X., Liu, M., Zhang, L., 2018. Co-adsorption and sequential adsorption of the co-existence four heavy metalions and three fluoroquinolones on the functionalized ferromagnetic 3D NiFe2O4 porous hollow microsphere. J. Colloid Interface Sci. 511, 135–144.
Mawad, A.M.M., Hesham, A.E.L., Khan, S., Nawab, J., 2020. The role of fungi and genes for the removal of environmental contaminants from water/wastewater treatment plants. In: Hesham, A.L., Upadhyay, R., Sharma, G., Manoharachary, C., Gupta, V. (Eds.), Fungal Biotechnology and Bioengineering. Fungal Biology. Springer.
Pohl, A., 2020. Removal of heavy metal ions from water and wastewaters by sulfur-containing precipitation agents. Water Air Soil Pollut. 231, 503.
Puszkarewicz, A., Kaleta, J., 2020. The efficiency of the removal of naphthalene from aqueous solutions by different adsorbents. Int. J. Environ. Res. Public. Health 17, 5969.
Rastegari, A.A., Yadav, A.N., Gupta, A., 2019. Prospects of Renewable Bioprocessing in Future Energy Systems. Springer International Publishing, Cham.
Raza, W., Lee, J., Raza, N., Luo, Y., Kim, K.H., Yang, J., 2019. Removal of phenolic compounds from industrial Wastewater based on membrane-based technologies. J. Ind. Eng. Chem. 71, 1–18.
Rekha, K.H., Lokeshappa, B., 2020. Comparative studies on removal of heavy metals from electroplating Wastewater through soil aquifer treatment (SAT) in conjunction with adsorbents. Water Sci. Technol. 82 (10), 2148–2158.
Samanta, M., Mitra, D., 2021. Treatment of petroleum hydrocarbon pollutants in water. In: Inamuddin, Ahamed, M.I., Lichtfouse, E. (Eds.), Water Pollution and Remediation: Organic Pollutants, Environmental Chemistry for a Sustainable World, 54. Springer, Cham.
Samson, R.A., Noonim, P., Meijer, M., Houbraken, J., Frisvad, J.C., Varga, J., 2007. Diagnostic tools to identify black aspergilli. Stud. Mycol. 59, 129–145.
Scimeca, M., Bischetti, S., Lamsira, H.K., Bonfiglio, R., Bonanno, E., 2018. Energy dispersive X-ray (EDX) microanalysis: a powerful tool in biomedical research and diagnosis. Eur. J. Histochem. 62 (1), 2841.
Sharma, K.R., Giri, R., Sharma, R.K., 2022. Efficient bioremediation of metal containing industrial wastewater using white rot fungi. Int. J. Environ. Sci. Technol.
Silva, T.L., Sousa, E., Pereira, P.T., Ferraò, A.M., Roseiro, J.C., 1998. Cellular fatty acid profiles for the differentiation of *Penicillium* species. FEMS (Fed. Eur. Microbiol. Soc.) Microbiol. Lett. 164, 303–310.
Simarro, R., González-Benítez, N., Bautista, L., Molina, M., 2013. Biodegradation of high-molecular-weight polycyclic aromatic hydrocarbons by a wood degrading bacterial consortium at low temperatures. FEMS (Fed. Eur. Microbiol. Soc.) Microbiol. Ecol. 83, 438–449.
Tamura, K., Peterson, D., Peterson, N., Stecher, G., Nei, M., Kumar, S., 2011. MEGA5: molecular evolutionary genetics analysis using likelihood, distance, and parsimony methods. Mol. Biol. Evol. 28 (10), 2731–2739.
Tiwari, K.L., Jadhav, S.K., Kumar, A., 2011. Morphological and molecular study of different *Penicillium* species. Middle East J. Sci. Res. 7 (2), 203–210.
Vacar, C.L., Covaci, E., Chakraborty, S., Li, B., Weindorf, D.C., Frentiu, T., Pârvu, M., Podar, D., 2021. Heavy metal-resistant filamentous fungi as potential mercury bioremediators. J. Fungi 7, 386.
Vahabisani, A., An, C., 2021. Use of biomass-derived adsorbents for the removal of petroleum pollutants from water: a mini-review. Environ. Syst. Res. 10, 25.
Varjani, S., Joshi, R., Srivastava, V.K., et al., 2020. Treatment of wastewater from petroleum industry: current practices and perspectives. Environ. Sci. Pollut. Res. 27, 27.
Wei, Y., Jin, Y., Zhang, W., 2020. Treatment of high-concentration wastewater from an oil and gas field via a paired sequencing batch and ceramic membrane reactor. Int. J. Environ. Res. Public Health 17, 1953.
White, T.J., Bruns, T.D., Lee, S.B., Taylor, J.W., 1990. Amplification and direct sequencing of fungal ribosomal RNA genes for phylogenetics. In: Innis, M.A., Gelfand, D.H., Sninsky, J.J., White, T.J. (Eds.), PCR Protocols: A Guide to Methods and Applications. Academic Press, New York, pp. 315–322.
World Health Organization (WHO), 2011. Guidelines for Drinking Water Quality, Recommendations, fourth ed., p. 541 Geneva, Switzerland, vol. 1.
Yue, J., Qinglin, X., Wenjie, Z., 2016. High-strength ethylene glycol wastewater treatment in anaerobic polyvinyl alcohol gel beads based biofilm reactor. Glob. NEST J. 18 (1), 46–54.
Zain, M.E., Bahkali, A.H., Al-Othman, M.R., 2013. Developments in using fatty acids in fungal chemotaxonomy. Afr. J. Microbiol. Res. 7 (38), 4638–4645.
Zhang, W., Xie, Q., Rouse, J.D., Qiao, S., Furukawa, K., 2009. Treatment of high-strength corn steep liquor using cultivated polyvinyl alcohol gel beads in an anaerobic fluidized-bed reactor. J. Biosci. Bioeng. 107, 49–53.
Zhang, W., Liu, F., Wang, D., Jin, Y., 2018. Impact of reactor configuration on treatment performance and microbial diversity in treating high-strength dyeing wastewater: anaerobic flat-sheet ceramic membrane bioreactor versus up flow anaerobic sludge blanket reactor. Bioresour. Technol. 269, 269–275.
Zhang, D., Yin, C., Abbas, N., et al., 2020. Multiple heavy metal tolerance and removal by an earthworm gut fungus *Trichoderma brevicompactum* QYCD-6. Sci. Rep. 10, 6940.